## THEORY OF ELECTRON TRANSFER REACTIONS AND COMPARISON WITH EXPERIMENTS\*

R. A. MARCUS and PRABHA SIDDARTH Noyes Laboratory of Chemical Physics 127-72 California Institute of Technology Pasadena CA 91125 USA

ABSTRACT. In these lectures, reaction rate theory and the theory of electron transfer (ET) reactions are outlined. The topics discussed include the relation of the potential energy surfaces to free energy curves for ET reactions, classical ET theory for reactions in solution and at interfaces, quantum corrections, the inverted effect, relation to charge transfer spectra, the cross-relation, adiabatic and nonadiabatic ET reactions, electronic matrix elements, relation to other transfer reactions, predictions of and comparison with experiments, and miscellaneous questions.

#### **OUTLINE**

Page			
50	1. Introduction		
51	2. Theory		
51		Potential Energy Surfaces and Free Energy Surfaces	
55	2.2	Classical Theory	
60		Electrochemical ET Reactions	
62	2.4	Predictions from Theory	
62		2.4.1 The inverted effect	
64		2.4.2 The cross-relation	
65		2.4.3 Electrochemical relationships	
65	2.5	Quantum Correction and Nuclear Tunneling	
69	2.6	Other	
69	3. Com	3. Comparison of Theory and Experiment	
69	3.1	Rate Constants	
69	3.2	Solvent Effect	
69	3.3	Cross-Relation	
70		The Inverted Effect	
70	3.5	Relation between Rate Constants and Equilibrium Constants	
70	3.6	Electrochemical ET Reactions	
71		Adiabatic vs Nonadiabatic ET	
72	3.8	Electronic Matrix Elements	
74	3.9	Extension to Biological Systems	

<sup>\*</sup> From lectures given by RAM at the NATO Summer School at Aussois, 1991.

<sup>4</sup> 

E. Kochanski (ed.), Photoprocesses in Transition Metal Complexes, Biosystems and Other Molecules. Experiment and Theory, 49–88.

<sup>© 1992</sup> Kluwer Academic Publishers. Printed in the Netherlands.

- Page 75 4. Miscellaneous Questions
  - 79 5. Other Topics
  - 79 Acknowledgment
  - 80 Appendix A. Rate Expressions for Adiabatic and Nonadiabatic Reactions
  - 82 Appendix B. The Reorganizational Free Energy G(q)
  - 83 Appendix C. Comparisons of Quantum Expressions and Remarks on  $\ln k_r vs \Delta G^0$  Asymmetry

### 1. Introduction

Electron transfer (ET) reactions play an important role in many chemical and biological reactions. The simplest of all ET reactions is the "self-exchange" reaction, as in the isotopic exchange reactions,

$$\operatorname{Fe}(\operatorname{CN})_{6}^{4-} + \operatorname{Fe}^{*}(\operatorname{CN})_{6}^{3-} \xrightarrow{k_{11}} \operatorname{Fe}(\operatorname{CN})_{6}^{3-} + \operatorname{Fe}^{*}(\operatorname{CN})_{6}^{4-}$$
 (1)

$$\operatorname{Ce}\left(\operatorname{IV}\right) + \operatorname{Ce}^{*}\left(\operatorname{III}\right) \qquad \stackrel{k_{22}}{\longrightarrow} \qquad \operatorname{Ce}\left(\operatorname{III}\right) + \operatorname{Ce}^{*}\left(\operatorname{IV}\right) \tag{2}$$

where the asterisk denotes a radioactive isotope. Since the products are chemically equivalent to the reactants, these reactions have a zero value for the standard free energy of reaction  $\Delta G^0$ . The study of their rates has provided, thereby, direct information on the "intrinsic" factors which control the rate of ET. When two different redox systems are involved, as in

$$Fe(CN)_6^{4-} + Ce(IV) \rightarrow Fe(CN)_6^{3-} + Ce(III)$$
(3)

the ET reaction is commonly termed a "cross-reaction." For the latter, the standard free energy of the reaction,  $\Delta G^0$ , which measures the stability of the products relative to those of the reactants in a precise thermodynamical way, is an additional factor which influences the rate of the ET reaction.

In addition to inorganic ET reactions in solution, studies in the ET field include a wide range of topics, including organic and biological ETs, thermal and photoinduced ETs, charge transfer spectra, and ET reactions at metal electrodes and at other types of interfaces, such as semiconductor-liquid, modified electrode-liquid, polymer-liquid and liquid-liquid interfaces, colloids and micelles. These areas and their connections are among those depicted in Figure 1. We review some essential features of the theory underlying ET reactions and then compare some of the theoretical predictions with the experimental results.

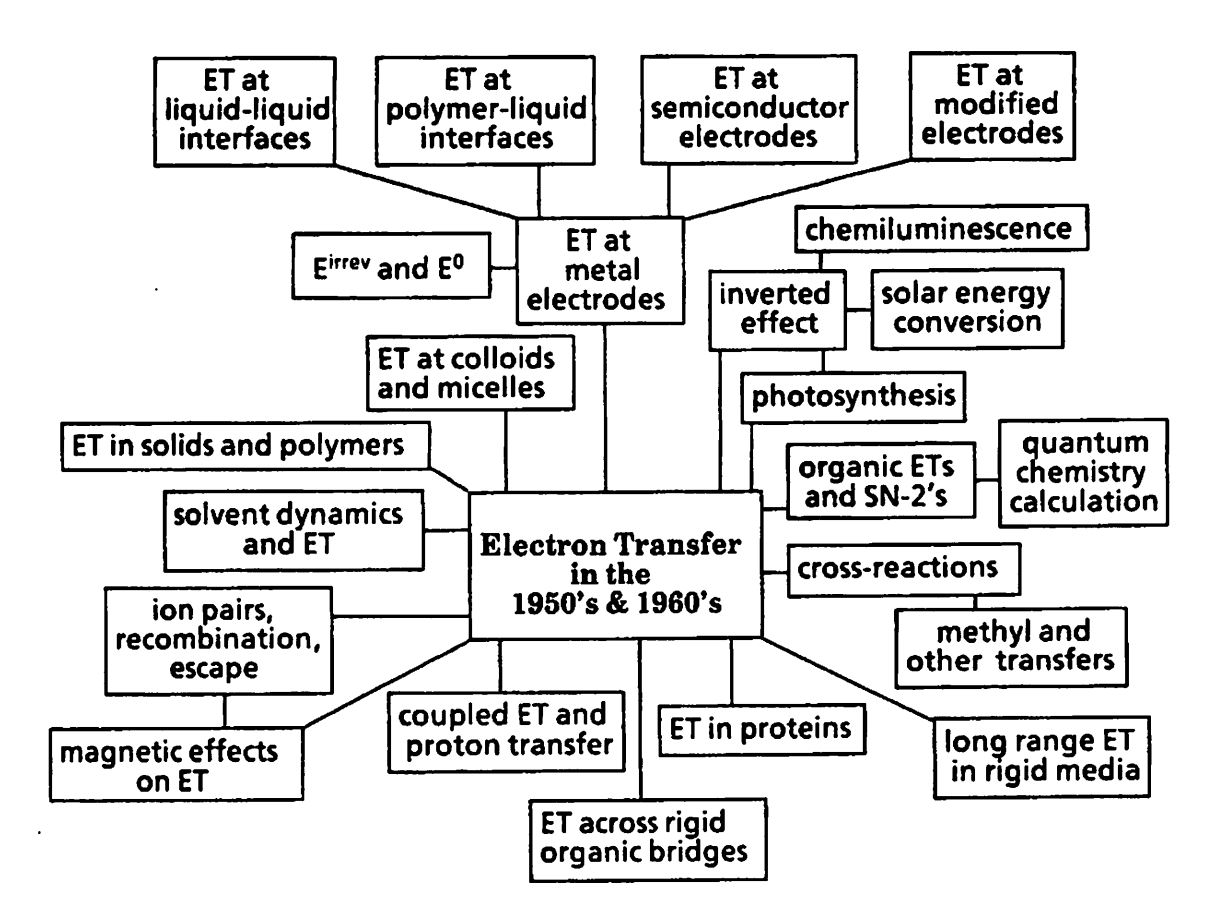


Figure 1. Examples of topics in the electron transfer field.

In general, we consider the ET reaction

$$(Ox)_1 + (Red)_2 \rightarrow (Red)_1 + (Ox)_2 \tag{4}$$

where the reactants may be moving freely in solution or may be attached to each other so that eq 4 then becomes an intramolecular ET.

### 2. Theory

### 2.1 POTENTIAL ENERGY SURFACES AND FREE ENERGY SURFACES

In reactions 1 to 3, the ET reaction is accompanied by changes in the nuclear configurations of the reactants and in the surrounding environment, such as changes in metal-ligand bond lengths in the reactants and changes in the typical orientations of the nearby dipolar solvent molecules. In the case of reaction 1, for example, each  $Fe^{2+}$ – $OH_2$  bond in aqueous solution is about 0.14 Å longer than the  $Fe^{3+}$ – $OH_2$  bond. This latter change imposes a barrier of

about 8 kcal mol<sup>-1</sup> to the reaction.<sup>10</sup> Further, solvent molecules are more oriented around the Fe<sup>3+</sup> ion than around the Fe<sup>2+</sup> ion, since the former is more highly charged, contributing approximately 8 kcal mol<sup>-1</sup> to the free energy barrier of the reaction<sup>10</sup>. Both effects are illustrated in Figure 2. In order for ET to occur, the reactants must approach each other and, at the same time, typical nuclear configurations of the reactants have to evolve toward those of the products by suitable fluctuations in the coordinates. In the present case, these coordinates are the vibrational modes of the reactants, the orientational coordinates of the surrounding solvent molecules, and, to some extent, the vibrational coordinates of the polarized solvent molecules.

### **Electron Transfer in Solution**

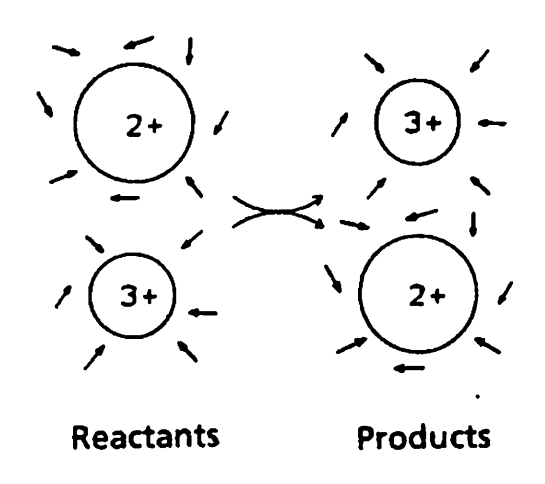


Figure 2. Typical nuclear configurations for reactants, products, and surrounding solvent molecules (cf. ref 11). The longer M-OH<sub>2</sub> bond length in the +2 state is indicated schematically by the larger ionic radius.

To treat the mechanism of ET, it is useful to consider the many-dimensional potential energy surface (PES) for the reactants and the surrounding medium,  $U_r$ , and that for the products and surrounding medium,  $U_p$ . These PES are a function of many (~thousands) of the solvent's and reactants' coordinates, say N. The intersection of these two PES forms an (N-1)-dimensional surface, which, because of the Franck-Condon principle discussed later, serves as the transition state for the reaction. A schematic one-dimensional profile of the two PES and their intersection is given by the solid lines in Figure 3. A somewhat more realistic but still schematic profile is shown by the dashed lines in Figure 3. The latter profile is more complicated, since the dependence of  $U_r$  and  $U_p$  on the solvational coordinates leads to many local potential energy minima. The dependence of  $U_r$  and  $U_p$  on the vibrational coordinates, on the other hand, is quadratic to a reasonable approximation for the energies of interest.

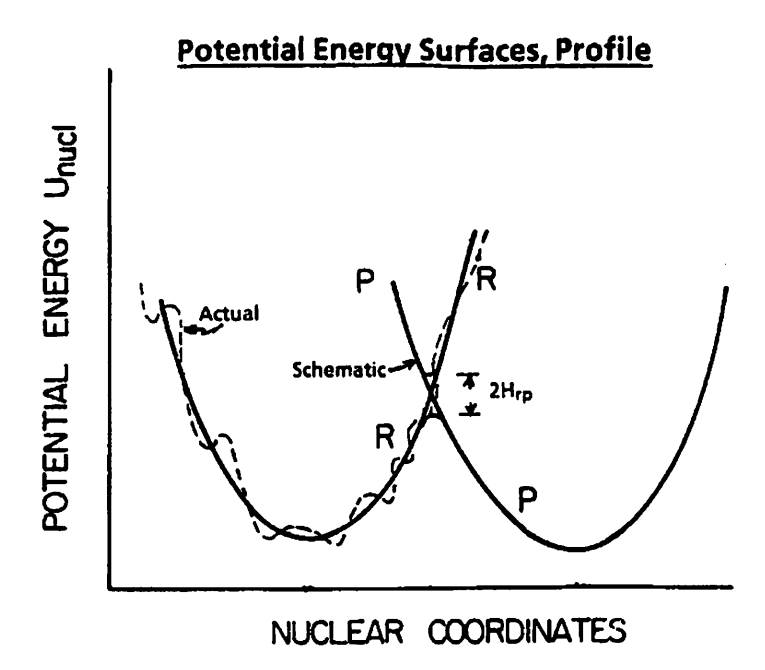


Figure 3. Profile of potential energy surfaces for reactants plus environment, R, and for products plus environment, P. Solid curves: highly schematic. Dashed curves: schematic but more realistic. The typical splitting,  $2H_{rp}$ , at the intersection of  $U_r$  and  $U_p$  is exaggerated in the Figure.

It is useful to consider first an intramolecular ET reaction, and the fluctuations in coordinates, at a fixed separation distance R between the electron donor and the acceptor. We subsequently include, in the case of bimolecular reactions, or in the case of an ET reaction between a freely moving reactant and an electrode, the role of the translational coordinates, which permit R to vary. Thus, in the following, the N coordinates first refer to those of a system in which the positions of the reactants, and hence R, are held fixed.

For ET reactions in which there is a weak electronic interaction between the reactants, a reaction coordinate q can be defined globally in a rather precise manner. The method of doing so would take us a little far afield, but is equivalent to using  $U_p - U_r$  as a coordinate (cf. ref 12 or an equivalent definition in ref 13). For any given value of q, the system resides on an (N-1)-dimensional surface in coordinate space, and the free energy,  $G_r(q)$ , for the reactants and their surrounding environment can be calculated for any value of q. The expression for  $G_r(q)$  contains the value of  $\exp\left[-U_r(q)/k_BT\right]$ , integrated over this (N-1)-coordinate surface, and also contains a momentum contribution and a factor  $h^{N-1}$ , h being Planck's constant, as in eq B2 of Appendix B. The last two factors, which are omitted here in the interests of notational brevity, cancel when a free energy difference  $\Delta G_r^*$  is later considered. We thus have

$$\exp\left[-G_r(q)/k_BT\right] = \int \dots \int \exp\left(-U_r(q)/k_BT\right)dS \tag{5}$$

where dS is a volume element in this (N-1)-dimensional space for fixed positions of the translational coordinates of the reactants.

In a linear response approximation, assumed in the theory,  $^{13-15}$  the contribution of the orientations of the solvent dipoles to changes in the solvent dielectric polarization is proportional to changes in the electric fields, and the approximation is sometimes referred to as the "dielectric unsaturation approximation." In this linear response regime,  $G_r(q)$  is then a quadratic function of q. Recent computer simulations have provided further support for the approximation.  $^{16}$   $G_r(q)$  and  $G_p(q)$  can thus be drawn as parabolas, as in Figure 4, even when  $U_r(q)$  and  $U_p(q)$  are highly anharmonic functions of many of the coordinates. The approximation is much less drastic than assuming that  $U_r(q)$  itself is a quadratic function of all the coordinates, collectively denoted here by q.

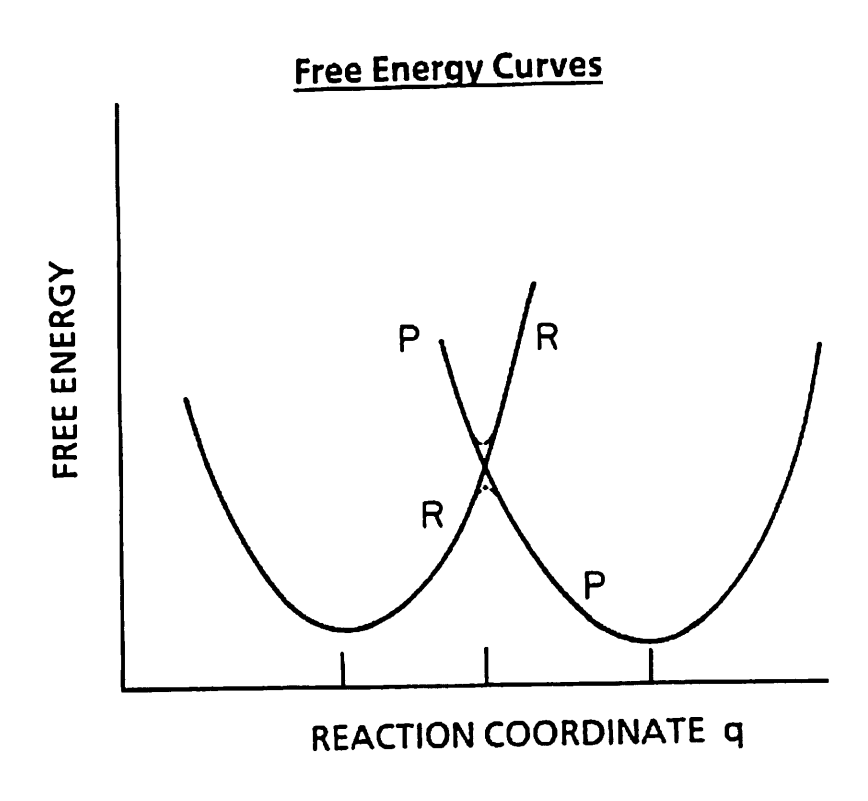


Figure 4. Free energy of reactants plus environment vs the reaction coordinate q (R curve), and free energy of products plus environment vs q (P curve). The three vertical lines on the abscissa denote, from left to right,  $q^r$ ,  $q^{\ddagger}$  and  $q^p$ .

For electron transfer to occur, one of the conditions which must be satisfied is the Franck-Condon principle. The latter may be described as follows, in terms of a classical description of the nuclear motion: Because the motion of the nuclei is typically slow compared with that of the electrons, the

nuclei change neither their instantaneous position nor their instantaneous momenta during an electronic transition. In the present case, this transition is one from the electronic configuration of the reactants to that of the products, and is the electron transfer. The only region in the N-dimensional coordinate space where the above conditions on coordinates and momenta can be satisfied in a thermal reaction is where  $U_r(\mathbf{q}) = U_p(\mathbf{q})$ , i.e., on the (N-1)-dimensional surface where the two surfaces  $U_r$  and  $U_p$  in N-dimensional coordinate space  $\mathbf{q}$  intersect. (In the profile of the N-dimensional system in Figure 3, this (N-1)-dimensional surface appears as a single point.) An electron transfer in any other region is a vertical transition in the Figure and can only occur upon the

absorption or emission of light.

This (N-1)-dimensional intersection surface, which is reached by a suitable thermal fluctuation of the coordinates, forms the transition state for this ET reaction. At the intersection, the system can go from the reactants' plus environment's potential energy surface  $U_r(\mathbf{q})$ , with a profile denoted there by R, to the products' surface P, if some electronic coupling exists between the two reactants. The extent of the coupling is indicated by the splitting  $2H_{rp}$  in Figure 3. When  $H_{rp}$  is large enough, the system will remain on the lower energy surface, i.e., go from the R surface to the P surface in the transition state region, with a probability of about unity each time the system crosses the intersection surface. The ET reaction is then said to be "adiabatic." If, on the other hand,  $H_{rp}$  is very small, for example when the two reactants are far apart, the system has only a small probability of reaching the P surface during this crossing of the TS, and the ET, if it occurs, is then said to be "nonadiabatic." A quantum mechanical-based expression for calculating this probability of transition from the  $U_r$  surface to the  $U_p$  one at the TS is sometimes employed, using the Landau-Zener expression,17 as described in Appendix A.

The calculation of the rate constant for an ET reaction thus involves calculating the probability of reaching the transition state multiplied by the probability of going from the R to the P surface in the transition state region. The probability of reaching the transition state can be expressed, in transition state theory, in terms of the free energy required to reach the transition state. We consider first the case where the nuclear motion is treated classically. Quantum mechanical corrections to the following are summarized briefly

later.

### 2.2 CLASSICAL THEORY

We consider either a system in which the donor and acceptor are held fixed at a separation distance R by some rigid molecular framework, or in which they are free to move in solution, approach each other and attain some typical separation distance R in the transition state. At this R we consider the free energy of fluctuations of the vibrational and solvational dipolar coordinates along a reaction coordinate q. There is also an additional free energy term in a bimolecular reaction, the "work" term  $w_r$  which is the change in free energy when the reactants fixed at some large separation distance are brought to the separation distance R. This  $w_r$  can have both electrostatic and nonelectrostatic contributions. In the interests of brevity of notation, we omit  $w_r$  and the corresponding term  $w_p$  for the products in the following expressions, although they are normally included in the expressions in the

literature. 1,15,18 We first give a quick derivation of an equation for the reorganizational free energy change needed to reach the TS, and then give a more detailed approach which expresses the reorganization parameter  $\lambda$  in terms of molecular properties.

An adiabatic reaction is considered first. In this case the rate constant,

written in terms of transition state theory (cf. Appendix A), is

$$k_r = \frac{k_B T}{h} \exp\left(-\Delta G^{\dagger} / k_B T\right) = \frac{k_B T}{h} \frac{Q^{\dagger}}{Q} \exp\left(-\Delta E_0^{\dagger} / k_B T\right)$$
 (6)

where  $Q^{\ddagger}$  is the partition function of the TS, Q is that of the reactants,  $\Delta G^{\ddagger}$  is the free energy of activation, and  $\Delta E_0^{\dagger}$  is the activation energy at 0° K. In a classical treatment, zero-point energies in  $\Delta E_0^{\dagger}$  vanish and the latter becomes  $\Delta U^{\dagger}$ , the lowest value of the potential energy in the TS minus that for the

reactants, as in eq A3 in Appendix A.

Upon integrating an expression for Q in Appendix B over all coordinates but the reaction coordinate q, a term  $\exp[-G(q)/k_BT]$  is obtained. In the linear response approximation G(q) is approximately a quadratic function of q. Combined with another term in Q arising from the momentum p conjugate to q, one factor contributing to Q in eq 6 is a classical harmonic oscillator partition function,  $k_BT/h\nu$ . Here,  $\nu$  is the typical frequency associated with motion along q (cf. eq 28 given later). A remaining factor in eq 6 is denoted by  $\exp(-\Delta G_r^*/k_BT)$ . For a unimolecular reaction, one then obtains from eq 6,  $k_r = v \exp(-\Delta G_r^*/k_BT)$ , as in Appendix A. Here,  $\Delta G_r^*$  is the free energy associated with the reorganization (fluctuations) of the solvent dipoles and of the vibrational coordinates needed to reach the TS. For bimolecular reactions, there are additional factors in  $Q^{\ddagger}$  and Q associated with the translational motion of the reactants and with their more restricted translational motion in the TS. The net result, derived in Appendix A, is included later in eq 14 for  $k_r$ .

The reorganizational free energy  $\Delta G_r^*$  required to reach the transition

state (TS) when the positions of the reactants are held fixed is

$$\Delta G_r^* = G_r(q^{\ddagger}) - G_r(q^r) \tag{7}$$

where  $G_r(q^{\ddagger})$  is the value of  $G_r(q)$  on the intersection surface (the TS) and  $q^r$ denotes the value of q for which  $G_r(q)$  has a minimum, as in Figure 4. An expression for  $\Delta G_r^*$  can be obtained using quadratic expressions for the free energies. We have

$$G_r(q) = \frac{k}{2} \left( q - q^r \right)^2 \tag{8a}$$

$$G_p(q) = \frac{k}{2} \left( q - q^p \right)^2 + \Delta G^o$$
 (8b)

where  $\Delta G^0$  is the standard free energy of the reaction, which also equals  $G_p(q^p) - G_r(q^r)$ .  $\Delta G_r^*$  is obtained as follows:

On the intersection surface the distribution of the coordinates and momenta is the same for the  $U_r$  and  $U_p$  surfaces. Thus, their entropies are the same for the R and P electronic states at the intersection surface. Similarly, the average of  $U_r$  over the coordinates defining the intersection surface equals the average of  $U_p$  there. Thus, we have  $U_p$ 

$$G_r(q^{\ddagger}) = G_p(q^{\ddagger}) \tag{9}$$

which together with eqs 7 and 8 yields

$$q^{\ddagger} = \frac{1}{2} (q^r + q^p) + \frac{\Delta G^0}{k (q^p - q^r)}$$
 (10)

These equations yield

$$\Delta G_r^* = \frac{\lambda}{4} \left( 1 + \frac{\Delta G^0}{\lambda} \right)^2 \tag{11}$$

where

$$\lambda = \frac{k}{2} \left( q^p - q^r \right)^2 \tag{12}$$

Using transition state theory, the net result for the rate constant  $k_r$  of the electron transfer reaction can be written as in eq 13a for a unimolecular reaction and in 13b for a bimolecular reaction (cf. Appendix A).

$$k_r = \kappa v \exp\left(-\Delta G_r^{\bullet}/k_B T\right) \tag{13a}$$

$$k_r = \kappa_V v_s \exp\left(-\Delta G_r^* / k_B T\right) \tag{13b}$$

where  $\Delta G_r^*$  is given by eq 11,  $\nu$  is the frequency associated with the motion along the q-coordinate, and v is the effective volume<sup>19</sup> which the reactants occupy in the TS, namely  $4\pi R^2/\beta$ , where  $\beta$  is the exponent in the dependence of the electron transfer rate on separation distance R (rate varies as  $\exp(-\beta R)$ ,  $\beta$  being about  $1\text{Å}^{-1}$ , depending on the system). The R in  $v_e$  is the mean separation distance in the TS. Equation 13b is of the same form as that given by Sutin.

For an adiabatic reaction the kv in eq 13 becomes v, while for a nonadiabatic reaction, it can be shown, as in Appendix A, to be given approximately by eq 14b:

$$\kappa v = v$$
 (adiabatic) (14a)

$$\kappa v = \frac{2\pi}{\hbar} \frac{|H_{rp}|^2}{\left(4\pi\lambda k_B T\right)^{1/2}} \quad \text{(nonadiabatic)}$$
 (14b)

The  $\lambda$  appearing in eq 12 is usually termed a reorganization energy and is the sum of  $\lambda_i$ , an inner (i.e., vibrational) contribution, and  $\lambda_o$ , an outer (i.e., solvational, outside any first coordination shell) contribution. The  $\lambda_i$  arises from vibrational motion of the nuclei of the reactants themselves, including those in any first coordination shell, and typically arises from any changes in bond lengths of each species when it is a product, as compared with when it is a reactant (eq 26 below). For example, for ET involving transition metal complexes, this  $\lambda_i$  would include the contribution from the metal atom-to-ligand coordinates. The  $\lambda_o$  includes the contributions from all the rest of the coordinates of the nuclei, which for ET reactions in solution means those of the solvent. We consider next a simple model which provides an estimate of  $\lambda$ .

The vibrations of each reactant are treated as normal modes of vibration. We let  $q_i$  denote the *i*th normal mode coordinate,  $q_i^r$  its equilibrium value for the reactants,  $q_i^p$  that for the products, and  $k_i$  the associated force constant  $4\pi^2v_i^2$ ,  $v_i$  being the normal mode frequency for that mode. The contribution from the reactants' vibrations to the potential energy of a fluctuation

 $U_i^{vib}(j=r,p)$  is

$$U_{j}^{vib} = \frac{1}{2} \sum_{i} k_{i} \left( q_{i} - q_{i}^{j} \right)^{2} , \qquad j = r, p$$
 (15)

The  $\Delta G_r$  in eq 13 contains a  $\Delta G_{solv}$  and a  $\Delta U_{vib}$ . (Vibrational entropic terms in this vibrational model can be shown to cancel in  $\Delta G_r$ , a more detailed derivation being given in the literature, 15 a result which can also be inferred

using expressions for Q and  $Q^{\ddagger}$  given in Appendix A.)

To express the "outer" contribution to G, we shall treat the solvent as a dielectric continuum and neglect dielectric image effects, which tend to be small for the interaction of the two charges in solution. A more general formulation is again available in refs 14 and 15. If P(r) denotes a particular function of the dielectric orientation polarization of the solvent at point r, then the free energy contribution  $G^{solv}$  due to these charge-charge and charge-solvent polarization interactions is given by  $P^{2}$ 

$$G_j^{solv} = -\frac{1}{8\pi} \left( 1 - \frac{1}{D_{op}} \right) \int D_j^2(\mathbf{r}) d\mathbf{r} - \int P \cdot D_j(\mathbf{r}) d\mathbf{r} + 2\pi c \int P^2 d\mathbf{r}$$
 (16)

where  $1/c = 1/D_{op} - 1/D_s$  and  $D_j(r)$  is the electric field associated with the charge distribution  $\rho_j$ .

$$D_{i}(\mathbf{r}) = -\nabla_{r} \int \rho_{i}(\mathbf{r}') / |\mathbf{r} - \mathbf{r}'| \, d\mathbf{r}' , \qquad j = r, p \qquad (17)$$

We now have

$$G_{r}(\mathbf{q},\mathbf{P}) = U_{r}^{vib}(\mathbf{q}) + G_{r}^{solv}(\mathbf{P})$$
 (18a)

and

$$G_p(\mathbf{q}, \mathbf{P}) = U_p^{vib}(\mathbf{q}) + G_p^{solv}(\mathbf{P}) + \Delta G^0$$
 (18b)

where q now denotes only the totality of the vibrational coordinates  $q_i$  rather than all the coordinates.

In order to find the values  $P^{\ddagger}(r)$  and  $q^{\ddagger}$  in the TS,  $G_r(q,P)$  is minimized with respect to variations in P(r) and q, subject to the condition that  $G_r(q,P)$  and  $G_p(q,P)$  are equal at the transition state:

$$G_{r}(\mathbf{q},\mathbf{P}) = G_{p}(\mathbf{q},\mathbf{P}) \tag{TS}$$

Thus,

$$\delta G_r = 0 \tag{20a}$$

subject to

$$\delta G_r - \delta G_p = 0 \tag{20b}$$

Equation 20 and use of a Lagrangian multiplier m yields, upon introduction of eqs 15, 16, 18 and 19,

$$4\pi c \mathbf{P}(\mathbf{r}) = \mathbf{D}_r(\mathbf{r}) + m \left[ \mathbf{D}_r(\mathbf{r}) - \mathbf{D}_p(\mathbf{r}) \right]$$
 (21)

and

$$q_i^{\dagger} = q_i^r + m(q_i^r - q_i^p) \tag{22}$$

Introducing these results into eqs 15 and 16, it follows that

$$\Delta G^* = \frac{\lambda}{4} \left( 1 + \frac{\Delta G^0}{\lambda} \right)^2 \tag{23}$$

where

$$\lambda = \lambda_{o} + \lambda_{i} \tag{24}$$

$$\lambda_o = \frac{1}{8\pi c} \int \left( D_r - D_p \right)^2 dr \qquad (25)$$

$$\lambda_i = \sum_{i=1}^{n} \frac{1}{2} k_i \left( q_i^p - q_i^r \right)^2 \tag{26}$$

If the two reactants can be treated as spherical, then  $\lambda_0$  is found to be given by<sup>14</sup>

$$\lambda_{o} = \left(\frac{1}{2a_{1}} + \frac{1}{2a_{2}} - \frac{1}{R}\right) \left(\frac{1}{D_{op}} - \frac{1}{D_{s}}\right) \tag{27}$$

where  $a_1$  and  $a_2$  are the radii of the two reactants, and R is their center-to-center separation distance. Models in which the pair of reactants is approximated by an ellipsoid have also been developed in the literature. The  $\nu$  in eq 14a is approximately given by  $^{26,\,27}$ 

$$v = \left(\sum_{k} \lambda_{k} v_{k}^{2} / \lambda\right)^{1/2} \qquad (k = i, o)$$
 (28)

using the notation in eq 24, or if there are several vibrational frequencies contributing to  $\lambda_i v_i^2$ , the sum in eq 28 is over all of them,  $\sum_j \lambda_j v_j^2 + \lambda_o v_o^2$ . The

often neglected  $v_o$  is associated with the "inertial motion" of the solvent. From eqs 23 to 27, it can be seen that  $\Delta G^*$  decreases with increasing  $a_1$  and  $a_2$ , decreasing R, increasing  $D_{op}$  and decreasing  $D_s$ . These observations can be physically interpreted as follows: (a) With increasing ionic radii  $a_1$  and  $a_2$ , the ion-solvent interactions decrease so that a smaller reorganization is needed for reaction and hence a smaller  $\lambda_o$ . (b) When the distance between the reactants is decreased, again there is less reorganization, since the somewhat distant solvent molecules can discriminate less between the two charge distributions when R is small, i.e., discriminate less between the charge distribution of the reactants and that of the products. Thereby, a smaller reorganization is needed and therefore a smaller  $\lambda_o$  occurs. (c) With a greater optical dielectric constant  $D_{op}$ , the electrostatic fields of the charges are more shielded and therefore the energy difference of ion-solvent interactions for the two charge distributions is less, leading to less reorganization. When  $D_s$  equals  $D_{op}$ ,  $\lambda_o$  is zero, the solvent now being nonpolar.

### 2.3 ELECTROCHEMICAL ET REACTIONS

Another class of ET reactions is that of electrochemical ET reactions. For the case of ET between an ion or a molecule and a metal electrode, a detailed analysis shows that in the usual region,  $[|ne(E-E_0')| < \lambda, \text{ in the notation used below]}$ , the transferring electron goes mainly from or into the Fermi level of the metal. 15,26,28,29 Also, now the metal electrode has densely spaced electronic states (a few are indicated schematically in Figure 5).

# Electrochemical Electron Transfer (Many electronic states in metal)

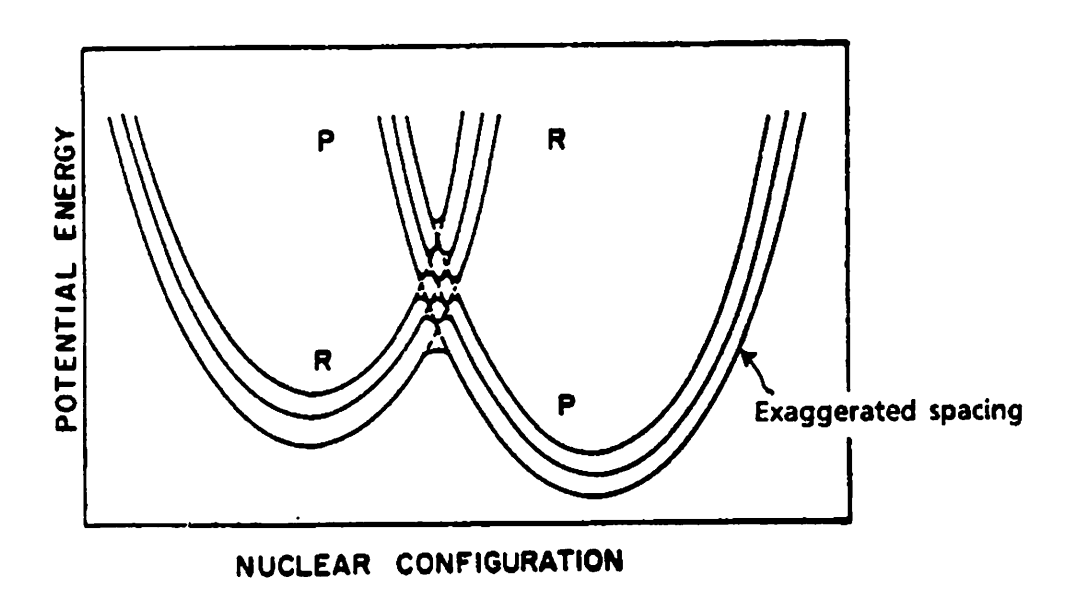


Figure 5. Potential energy profiles for reactants' system R (including electrode and solvent environment) and for products' system P for reaction 32. Several of the continuum of energy levels are depicted, with greatly exaggerated spacing.

Proceeding as before, eq 8 can now be written as

$$G^{r}(q) = \frac{k}{2} \left( q - q^{r} \right)^{2} \tag{29}$$

$$G^{p}(q) = \frac{k}{2} \left( q - q^{p} \right)^{2} + ne \left( E - E_{0}' \right)$$
 (30)

upon following the arguments given in refs 15 and 28. Here, E is the half-cell potential,  $E_0$ ' is the "standard" half-cell potential in the prevailing medium, and n is the number of electrons of charge e transferred between reactant and electrode. Thus  $n(E-E_0)$ , the activation overpotential, plays the same role as  $\Delta G^0$  in eq 7. 15,28,30

In the transition state we have, as before,

$$G^{r}(q^{\ddagger}, E_{0}') = G^{p}(q^{\ddagger}, E_{0}')$$
(31)

One ultimately obtains for the rate constant for the electrochemical reaction

$$Ox + M(ne) \rightarrow Red \tag{32}$$

the expression (cf. also Appendix A) given by eq 33a when the reactant moves freely in solution and by eq 33b when it is bound to the electrode.

$$k_{el} = \kappa v v_e e^{-\Delta G_{el}^* / k_B T}$$
 (33a)

$$k_{el} = \kappa v e^{-\Delta G_{el}^*/k_B T}$$
 (33b)

where  $k_{el}$ , the rate constant, is the rate per unit concentration of reactant per unit area of electrode.) In eq 33,  $\kappa\nu$  has the same meaning as in eqs 14a and 14b for the adiabatic and nonadiabatic limits,  $v_e$  is an effective volume, per unit area of electrode, from which electron transfer can occur ( $\approx \beta^{-1}$ , where  $\beta$  was the exponent defined in Section 2.2), and  $\Delta G_{el}$  is given by

$$\Delta G_{el}^{\bullet} \simeq \frac{\lambda_{el}}{4} \left[ 1 + \frac{ne\left(E - E_{0}'\right)}{\lambda_{el}} \right]^{2} \tag{34}$$

 $\lambda_{el}$  is given by equations similar to eqs 24 to 26, but now the sum in eq 26 is over the normal modes of the single reactant, and in eq 25 the expressions for  $\mathbf{D}_r(\mathbf{r})$  and  $\mathbf{D}_p(\mathbf{r})$  now take explicit account of the boundary conditions at the metal-liquid interface, utilizing, for example, the customary image charge description. When the reactant, denoted by 1, is treated as a sphere of radius  $a_1$ ,  $\lambda_o$  is given for the electrochemical ET by  $^{15,28}$ 

$$\lambda_{o,el} = \left(\frac{1}{2a_1} - \frac{1}{R}\right) (ne)^2 \left(\frac{1}{D_{op}} - \frac{1}{D_s}\right)$$
 (35)

where R is now twice the distance from the center of the reactant to the

electrode, in the transition state.

When the two reactants in a bimolecular reaction are in contact in the transition state, the R in eq 27 is approximately equal to  $a_1 + a_2$ . When the reactant in the electrochemical case is in contact with the metal electrode, in the transition state, the R in eq 35 is approximately  $2a_1$ . The  $\lambda_o$  for the electrochemical reaction is then seen from eqs 27 and 35 to equal half the  $\lambda_o$  for the self-exchange reaction. Further, the  $\lambda_i$  for the electrochemical reaction is one half the  $\lambda_i$  for the self-exchange reaction, there being only one half the number of vibrational normal modes undergoing changes. Thus the total  $\lambda$ 's then satisfy

$$\lambda_{el} \simeq \frac{1}{2} \lambda_{11} \tag{36}$$

However, when there is an adsorbed solvent layer on the electrode which the reactant cannot readily enter, then eq 36 is replaced by the inequality  $\lambda_{el} > \lambda_{11}/2$ . Consequences of eqs 33 to 36 are given later. If the reactant were bound to the electrode, instead of being free to move in solution, eq 36 would remain applicable only if the dielectric aspects were similar in the two systems and if the R in eq 27 were equal to the R in eq 35.

### 2.4 PREDICTIONS FROM THEORY

2.4.1 The inverted effect. From eq 23, it can be seen that when  $\Delta G^0$  is made increasingly negative at constant  $\lambda$ , the free energy barrier  $\Delta G^*$  initially decreases, and becomes equal to zero when  $-\Delta G^0 = \lambda$ . Upon making  $\Delta G^0$  more negative,  $-\Delta G^0$  then exceeds  $\lambda$ , and it is seen from eq 23 that the barrier begins to increase. In summary, the theory predicts that with an increase in  $-\Delta G^0$ , the rate will increase, reach a maximum, and then decrease, as in Figure 6. The regions where  $|\Delta G^0| < \lambda$  and  $|\Delta G^0| > \lambda$  are known as the "normal" and "inverted" regions, 13, 15 respectively (the regions I and III in Figure 6).

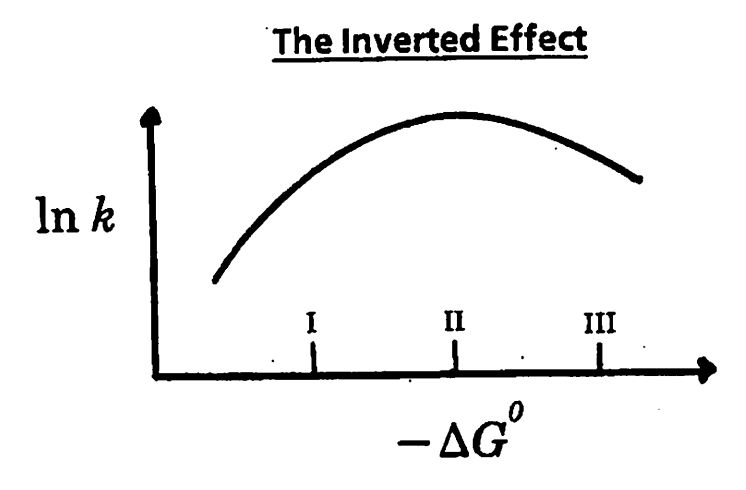
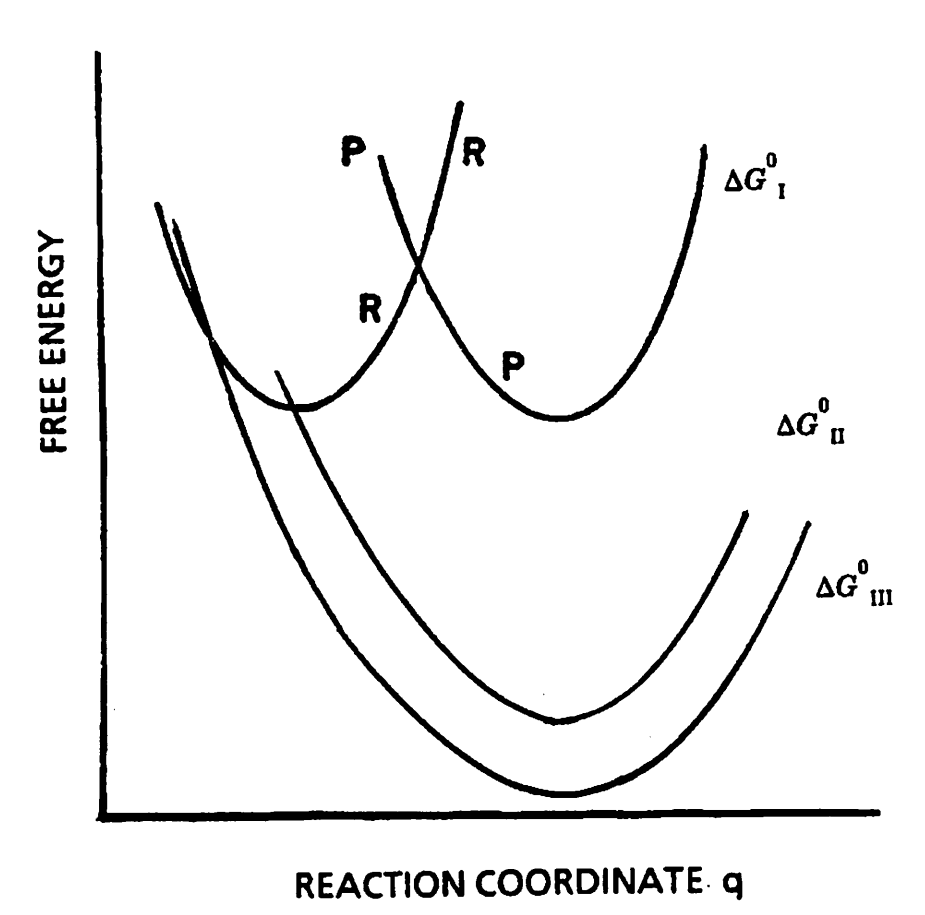


Figure 6. Plot  $\ln k_r vs - \Delta G^0$ . Points I and III are in the normal and inverted regions, respectively, while point II, where  $\ln k_r$  is a maximum, occurs when  $-\Delta G^0 = \lambda$ .

 $\Delta G^0$  can often be made increasingly negative by suitably changing the ligands of a reactant. This decrease in  $\Delta G^0$  corresponds to lowering the free energy surface of the products vertically in Figure 4. When this lowering is performed in small decrements, then at some  $\Delta G^0$ , namely, at  $\Delta G^0 = -\lambda$ , the intersection of the R and P free energy curves will occur at the minimum of the R curve (curve II in Figure 7). The reaction is then barrierless, i.e.,  $\Delta G^* = 0$ , and the rate constant is a maximum for the given  $\lambda$  (Figure 6). A further lowering of the P surface increases the free energy at the intersection and results in the inverted effect on the rate constant (curve III in Figure 7).



Plot of the free energy G versus the reaction coordinate q, for reactant (R) and product (P) systems, for the cases I to  $\coprod$ indicated in Figure 6.

Nuclear tunneling yields higher rates than would be predicted by the classical theory alone. The tunneling has a larger effect in the inverted region than in the normal region, because the effective barrier is "narrower" in the latter, as can be seen later in Figure 9. This result has the effect of distorting somewhat the  $\ln k_r vs \Delta G^0$  curve in Figure 7, so that the curve becomes asymmetric when nuclear tunneling occurs. Nevertheless, the maximum in the  $\ln k_r vs - \Delta G^0$  curve still occurs at  $-\Delta G^0 \sim \lambda$ .

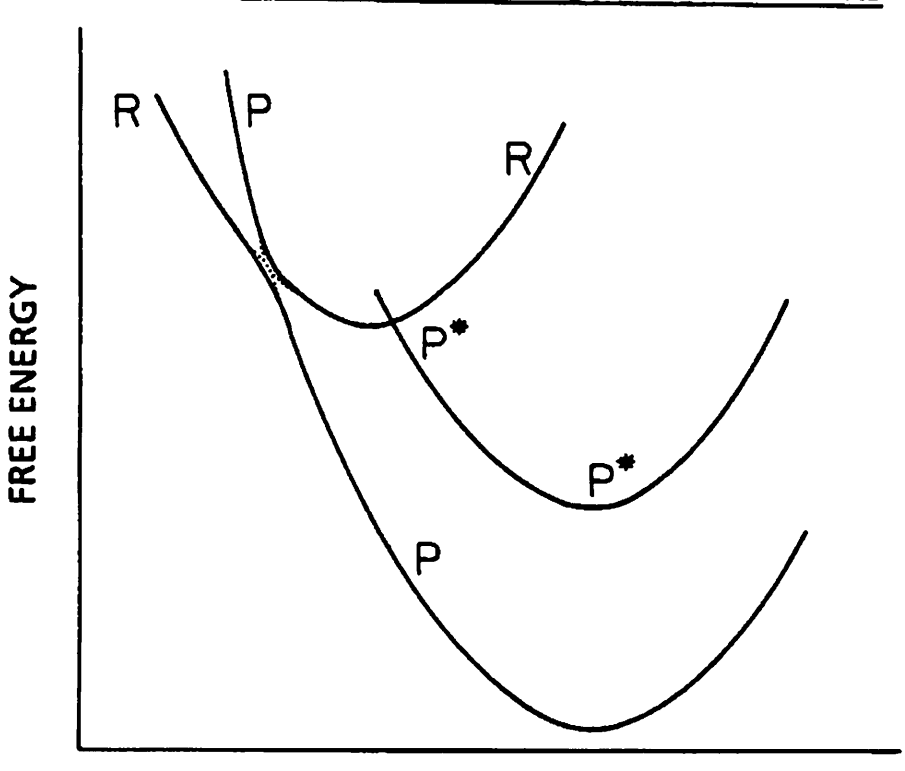
As noted in Section 2.5 and as has been described in ref 92, there is a parallelism between a  $k_r vs$  - $\Delta G^0$  plot and a charge transfer absorption or emission spectral plot. On one side of the spectral maximum, the

correspondence is to the "normal" region, and on the other, to the "inverted"

region

The inverted behavior is sometimes also seen in the preferential formation of an electronically excited product.  $^{31,32}$  Even though the intersection of the ground electronic state free energy curve P of the products and that of the reactants R may occur only at high energies in some cases, and so correspond to the reaction's being in the inverted region, an electronically excited-state free energy curve  $P^*$  of the products may intersect the R curve in a more favorable region, as in Figure 8. Then, this electronically excited state may form preferentially. This state can then either emit light, or form other states which emit light, or become deactivated. In this way, the ET reaction has resulted in a chemiluminescence.

### **Formation of Electronically Excited Products**



### **REACTION COORDINATE q**

Figure 8. Illustration of the case where the free energy curve G(q) for the reactants intersects at a low point the free energy curve for a products system  $P^*$  in which a product is electronically excited. In contrast, for the system depicted, the free energy barrier is higher for formation of products P in their ground electronic states.

2.4.2 The cross-relation. By noting that  $\lambda$  for a cross-reaction (such as eq 3) is approximately the average of the  $\lambda$ 's of the self-exchange reactions (in the present case, eqs 1 and 2), 15

$$\lambda_{12} = \frac{1}{2} \left( \lambda_{11} + \lambda_{22} \right) \tag{37}$$

the "cross-relation" for rate constants follows from eqs 13 and 23 for the case that the k in eq 13 is roughly unity for the reactions involved:15

$$k_{12} = \left(k_{11} k_{22} K_{12} f_{12}\right)^{1/2} \tag{38a}$$

where  $K_{12} = \exp(-\Delta G^0/k_BT)$ , the equilibrium constant of the reaction, and  $f_{12}$  is a known function of  $k_{11}$ ,  $k_{22}$  and  $K_{12}$ :

$$\ln f_{12} = \left(\ln K_{12}\right)^2 / 4 \ln \left(k_{11} k_{22} / v^2 v_s^2\right)$$
 (38b)

If, instead, the  $\kappa$  in eq 13 were substantially less than unity for the reactions involved, and if it were assumed that  $\kappa_{12} = (\kappa_{11} \kappa_{22})^{1/2}$ , then eq 38 would again be obtained, with the  $\nu^2$  in eq 38b now replaced by  $(\kappa_{11}\nu)(\kappa_{22}\nu)$ . In practice,  $f_{12}$  is usually close to unity.

2.4.3 Electrochemical relationships. When the k's in eqs 13a and 33a are approximately unity, the rate constant  $k_{ex}$  for self-exchange in solution, and the electrochemical rate constant  $k_{el}$  excorresponding to the so-called exchange current, namely at  $E = E_0$ , are related by

$$\left(k_{ex}/A_{ex}\right)^{1/2} \approx k_{el}^{ex}/A_{el} \tag{39}$$

upon using eq 36. Here,  $A_{ex}$  is the pre-exponential factor in  $k_{ex}$  (namely  $v_s v_s$ , which is roughly equal to  $10^{11}$  to  $10^{12}$  M<sup>-1</sup>s<sup>-1</sup>) and  $A_{el}$  is that in  $k_{el}$  (namely  $v_e v_s$  and which is roughly equal to  $10^4$  to  $10^5$  cm s<sup>-1</sup>).

An important difference, however, between electrochemical ET at metal

electrodes and ET in solution is that no inverted effect should occur for the former, since the transferring electron can always go into a high-energy unoccupied level of the metal instead of into a level near the Fermi level, or if the electron transfer is from the metal, it can always come from an occupied level of the metal well below the Fermi level instead of from a level near the Fermi level. In the case of a semiconductor, which has a narrow energy band instead of the very broad one in a metal, the inverted effect again becomes possible.

Another relationship is the dependence of  $\ln k_{el}$  on the activation overpotential  $ne(E-E_0)$ , given by eqs 33 and 34. It is analogous to the relation given in eqs 11 and 13 for the dependence of  $\ln k_r$  on  $\Delta G^0$  for a series of

homogeneous reactions having a constant  $\lambda$ .

### 2.5 QUANTUM CORRECTION AND NUCLEAR TUNNELING

In the formulation given above for the rate constant of an ET reaction, the nuclear motion was treated classically. However, there may be some nuclear tunneling through the barrier in Figure 3. The nuclear motion in the ET is described quantum mechanically in such cases. When the reaction is

nonadiabatic, the appropriate quantum mechanical expression is obtained using low order time-dependent perturbation theory, namely the Fermi golden rule expression.<sup>29,33</sup> The result is given by

$$k_r = \frac{2\pi}{\hbar} |H_{rp}|^2 (FC) \tag{40}$$

when the reactants are held fixed in position. Here, FC is a "Franck-Condon" factor involving the sum of products of overlap integrals of the vibrational and solvational wavefunctions of the reactants (and solvent) with those of the products, weighted by Boltzmann factors for the given temperature of the system. As before,  $H_{rp}$  is the electronic matrix element in Figure 3.

To obtain an expression for FC, one can either attempt to treat all coordinates, vibrational and solvational, quantum mechanically, or treat the higher-frequency vibrations of the inner shell coordinates quantum mechanically and treat the low-frequency modes of the system classically using for the latter the free energy of solvent reorganization given above. This approach also yields, in the high-temperature limit, 33-35 the expression (cf. Appendix A)

$$k_r = \frac{2\pi}{\hbar} |H_{rp}|^2 \frac{1}{\left(4\pi\lambda k_B T\right)^{1/2}} \exp\left[-\left(\Delta G^0 + \lambda\right)^2 / 4\lambda k_B T\right] \quad \text{(nonadiabatic)} \quad \text{(41)}$$

an expression which has also been derived using semiclassical theory.<sup>36</sup> The pre-exponential factor in eq 41 corresponds to the  $\kappa\nu$  in eq 13a, for this case that  $\kappa<<1$ , as already noted in eq 14b.

Several of the quantum expressions which have been introduced for  $k_r$  are given below, for the case where the reaction is treated, in addition, nonadiabatically. The simplest of these expressions is the one-frequency model<sup>29</sup>

$$k_r = \frac{2\pi}{\hbar} |H_{rp}|^2 \frac{1}{h\nu} \exp(py - S \coth y) I_p(S \operatorname{cosech} y)$$
 (42)

where  $S = \lambda_i/h\nu$ ,  $\nu$  is a vibration frequency, regarded as some mean frequency for all vibrations of the reactants and also for the solvent, the solvent being treated as a collection of oscillators, all of this same frequency  $\nu$ .  $I_p$  is a modified Bessel function of the first kind,  $p = -\Delta G^0/h\nu$ , and  $y = h\nu/2k_pT$ .

modified Bessel function of the first kind,  $p = -\Delta G^0/h\nu$ , and  $y = h\nu/2k_BT$ . A more general quantum expression is one where all high frequency vibrations are treated as having a single frequency  $\nu$ , while the remaining motion, including that of the solvent, is treated classically. For the case that  $h\nu/k_BT$  is so large that the reaction occurs mainly from the lowest vibrational state of the reactants, we have<sup>33</sup>

$$k_{r} = \frac{2\pi}{\hbar} |H_{rp}|^{2} \frac{1}{\left(4\pi\lambda_{0}k_{B}T\right)^{1/2}} \sum_{m=0}^{\infty} \exp\left[-\left(\lambda_{0} + \Delta G^{0} + mhv\right)^{2}/4\lambda_{0}k_{B}T\right] e^{-S}S^{m}/m!$$
 (43a)

where m denotes an integer (not to be confused with the m in eq 21). For the more general case where the initial vibrational states may be thermally populated, instead of the system's being only in the lowest vibrational state, eq 43a would be replaced by<sup>33</sup>

$$k_r = \frac{2\pi}{\hbar} |H_{rp}|^2 \frac{1}{\left(4\pi\lambda_0 k_B T\right)^{1/2}} \sum_{m=-\infty}^{\infty} \exp\left[-\left(\lambda_0 + \Delta G^0 + mhv\right)^2 / 4\lambda_0 k_B T\right] \times \exp\left(my - S \coth y\right) I_m(S \operatorname{cosech} y) \tag{43b}$$

where y has the same significance as in eq 42. At moderate T, eq 43b reduces

to eq 43a, while at sufficiently high T, it reduces to eq 41.

We have discussed elsewhere  $^{92}$  the relationship between the  $k_r$  vs  $-\Delta G^0$  (not  $\ln k_r$  vs  $-\Delta G^0$ ) curve and the plot of charge transfer absorption ( $\epsilon_{v_a}/v_a$ ) or emission ( $f_{v_e}/v_e^3$ ) intensity vs frequency, ( $v_{a,e}-v^{max}$ ) curve. The spectral plot on one side of the maximum  $v^{max}$  corresponds to the "normal" region for  $k_r$ , while that on the other side of  $v^{max}$  corresponds to the inverted region. The spectral plot may show evidence of vibrational structure, and it is this structure which corresponds to the different m's in eq 43b. If  $\lambda_0$  were small enough, eq 43b would display a series of sharp peaks as a function of  $-\Delta G^0$ , peaks separated by the vibrational energy spacing hv. Instead, there is not merely one mode but others also, treated in eq 43b only by a classical term containing  $\lambda_0$ , and the broadening for each such "line" is given by the Gaussian factor in eqs 43a and 43b. In the regime where most of the broadening is due to fairly high frequencies (but not as high as the principal one, v in eqs 43), it may be necessary meanwhile to replace the temperature-dependent Gaussian factor in eqs 43 by a more general theoretically-based one containing these vibrations and so showing less temperature dependence.

We comment in Appendix C on the relationship between eqs 42 and 43a when both  $\lambda_0$  and T both tend to zero, and between eqs 42 and 43b when only  $\lambda_0$  tends to zero. In eqs 43a and 43b the significance of m is that it is the number of vibrational quanta in the products immediately after the ET minus that in

the reactants just before the ET. Equations 43a and 43b reflect the distribution of such m's.

When  $h \nu/k_B T$  is large, a linear dependence of  $\ln k_r$  on  $\Delta G^0$  tends to occur in the inverted region, for example as in ref 37, paralleling results on the energy gap law for radiationless transitions.<sup>38</sup> We comment on this linear dependence in Appendix C. There have been a number (e.g., ref 37) of applications of formulae related to or obtained from eq 43, for systems with high frequency vibrations (e.g., the relevant such modes invoked have frequencies around  $1000 \, \mathrm{cm}^{-1}$  to  $1500 \, \mathrm{cm}^{-1}$ ). Further, in the inverted region the rate constant  $k_r$  tends to become largely temperature-independent when the participating vibrations have high frequencies, as for example in ref 39, because the reaction then largely occurs from the lowest vibrational state of the reactants.

When the quantum effects of the nuclear motion are significant, the  $k_r$  is higher than that calculated classically. A useful interpretation can be given in terms of nuclear tunneling. To this end, the Franck-Condon factors are first expressed in terms of semiclassical theory, expressions which in the nuclear

tunneling regime are the exponentials given in Figure 9. They may be described as follows: We consider the case of tunneling along a vibrational coordinate x from an initial vibrational state  $n_r$  of the reactants to a vibrational state  $n_p$  of the products;  $n_p - n_r$  is equivalent to the m in eq 43. In Figure 9 the minimum of the vibrational curve  $U_r^{vib}$  is higher than that of the  $U_p^{vib}$  curve by an amount mhv. The semiclassical value of the vibrational state-to-state Franck-Condon factor is given in Figure 9, apart from a pre-exponential factor, for two cases, one where the slopes of  $U_r^{vib}$  and  $U_p^{vib}$  at the intersection have the same signs, and one where they have opposite signs. Each exponential is the semiclassical (also known as WKB) nuclear tunneling probability per encounter of the system with the barrier. In the diagram, the system strikes the barrier once during a period 1/v of the nuclear motion. In Figure 9,  $U_r^{vib}$  and  $U_p^{vib}$  are denoted by  $U_r$  and  $U_p$ .

### **Tunneling Factor**

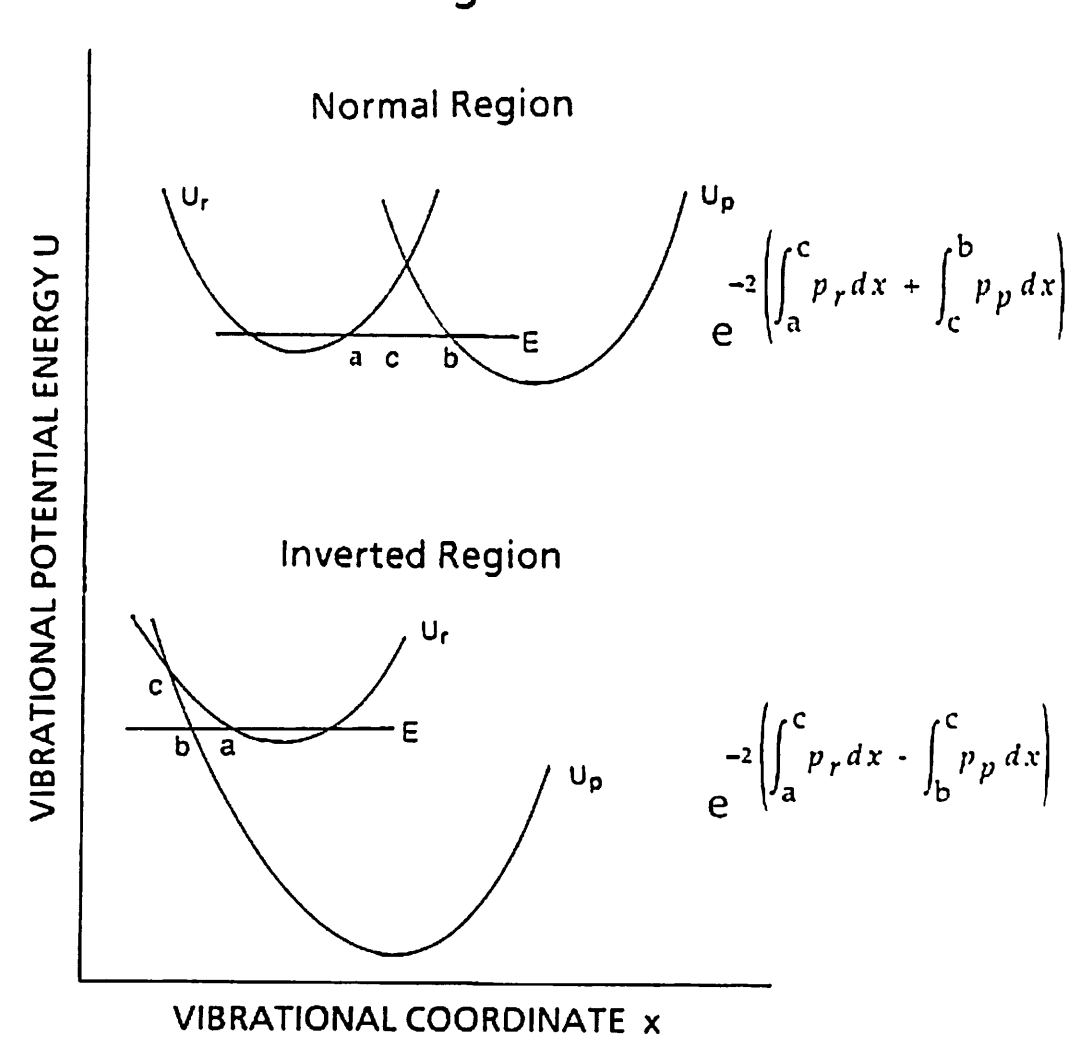


Figure 9. Nuclear tunneling in the normal and inverted regions. Indicated are profiles of the vibrational potential energy  $U^{vib}$  vs a vibrational coordinate x. The  $p_r(p_p)$  is the momentum along x when the system is on the  $U_r(U_p)$  curve. The vertical difference of the minima is the mhv in eqs 43.

#### 2.6 OTHER

ET theory has also been extended to ET's at various other types of interfaces (e.g., at semiconductor-liquid interfaces at modified electrodes, and at the interface of two immiscible liquids, and at other types of interfaces, involving polymers, for example), charge transfer spectra, and to a variety of other topics, some of which are included in Figure 1. However, in the interests of brevity, a discussion of these topics is omitted here.

### 3. Comparison of Theory and Experiment

Several applications of the theory outlined in the previous section, are summarized briefly in these notes, though they were described more fully in the lectures themselves.

#### 3.1 RATE CONSTANTS

An example of a comparison of measured self-exchange rate constants with those calculated using eqs 13a and 23 to 27, is given in Table VI of ref 4. The general agreement between theory and experiment is surprisingly good, particularly considering that the rate constants themselves span a wide range of values (from  $10^{-9}$  to  $10^{9}$ ).

#### 3.2 SOLVENT EFFECT

The theory predicts a dependence of the ET rates on the solvent dielectric properties via eq 27. Example of a plot of  $\log k$  versus  $(1/D_{op}-1/D_s)$  for the bis (biphenyl) chromium +/- exchange is given in ref. 41. The plot shows the predicted linear dependence of the logarithm of rate on  $(1/D_{op}-1/D_s)$ . However, such a good correlation is not always found, and factors such as ion-pairing, specific solvation effects and strong interaction between reactants can cause unexpected solvent dependences. Additional tests have been made using the solvent dependence of the absorption or emission maximum of charge transfer spectra, e.g., as in the plot<sup>42</sup> for [(bipy)<sub>2</sub> Cl Ru<sup>II</sup> L Ru<sup>III</sup> Cl (bipy)<sub>2</sub>]<sup>3+</sup>, where the ligand L is varied.

### 3.3 CROSS-RELATION

There have been numerous experimental tests of the cross-relation, eq 38, some of which are shown in Table I of ref 1. The agreement between theory and experiment in most cases is usually good, to within an order of magnitude. Deviations from the cross-relation can result when the driving force is large or when there is a change in mechanism for the self-exchange reactions and the cross-reaction, or when the work terms (not shown in eqs 11 and 13b) do not approximately cancel. In some instances, when a significant discrepancy between the observed and the calculated rate constants exists, this discrepancy has been taken as evidence for the operation of a special mechanism for one of these reactions being compared.

### 3.4 THE INVERTED EFFECT

The inverted region, <sup>13</sup> depicted in Figure 6, was not observed experimentally for many years. <sup>43</sup> The masking of the inverted effect could have many causes. Experiments that measure the rate of ET by quenching mechanisms may have sometimes given misleading results because quenching by more than one route is possible. (Other alternative routes, besides ET, for quenching are the formation of exciplexes <sup>44</sup> and the competition with other reaction mechanisms.) For ET reactions in solution, the behavior of the rate of ET near the maximum rate can also be masked by diffusion-control.

In recent years, however, the inverted behavior has been experimentally demonstrated in many cases, the first detailed such experiment being that of Miller, Closs and Calcaterra. It involved intramolecular ET for a series of compounds containing two molecular groups with different electron affinities, separated by a rigid bridge B, D-B-A. By varying either of the end groups, a range of  $\Delta G^{0}$ 's was achieved. Pulse radiolysis was used to generate electrons that were then trapped by the model compounds. The subsequent rate of transfer of electron (corrected for any intermolecular ET), plotted as a function of the standard free energy of the reaction, is shown in Figure 1 of ref 45 and clearly displays the inverted region.

According to the theory, the maximum rate of ET occurs when  $-\Delta G^0 = \lambda$ . It would require less energy to reorganize a nonpolar solvent than it would take to reorganize a polar solvent, and so  $\lambda$  would be smaller in the nonpolar case. Therefore, as a further test, the authors repeated their experiments in a nonpolar solvent, iso-octane, and compared their results with the experiments in MTHF. The maximum of the curve tended to be shifted to lower energy in iso-octane as predicted by the theory. Other results which demonstrate the

inverted effect include those in refs 46-49.

# 3.5 RELATION BETWEEN RATE CONSTANTS AND EQUILIBRIUM CONSTANTS

For a series of similar ET reactions (constant  $\lambda$ ), a plot of log of the rate constant  $k_r$  vs the log of the equilibrium constant K is expected to be curved, and the slope  $\alpha$  at any particular value of  $\Delta G^0$  is given by (from eqs 11 to 13)

$$\alpha = \frac{1}{2} \left( 1 + \frac{\Delta G^0}{\lambda} \right) \tag{44}$$

When  $|\Delta G^0| << \lambda$ , an approximate linear relationship between  $\log k$  and  $\log K$  results, with  $\alpha \approx 1/2$ . The slopes of plots of  $\log k$  vs  $\log K$  for some reactions are listed in Table III of ref 1, and in many cases a slope close to 0.5 is indeed observed.

### 3.6 ELECTROCHEMICAL ET REACTIONS

Many comparisons of the self-exchange rates with the rates of the corresponding reactions at an electrode have been made in order to test eq 43. A plot of  $\log k_{ex}$  vs  $\log k_{el}$  for some illustrative examples is given in Figure 6.10 of ref 6. The correlation is fairly good, but the electrochemical rates

appear to level off at higher rates. This may be a real discrepancy or may be an experimental problem, since at higher electrochemical rates, the reactive contribution to the measured A.C. impedance becomes smaller. There have been some recent attempts to make very small electrochemical devices in order to overcome this difficulty, and work is in progress.<sup>50</sup>

Studies of the effect of activation overpotential on the electrochemical ET

rate constant consistent with eq 34 have been described. 51,52

### 3.7 ADIABATIC us NONADIABATIC ET

The question of whether or not a particular electron transfer process is adiabatic, i.e., occurs at essentially every crossing of the TS, or nonadiabatic, i.e., rarely occurs during a crossing of the TS, is frequently encountered. It has

been possible to answer this question in some specific situations.

This question influences, via the  $\kappa$  in eq 33, the numerical value of  $A_{el}$  in eq 39. In a study of an electrochemical ET, the electron transfer "exchange current" and, thereby  $k_{el}^{ex}$ , was measured for the Ru(NH<sub>3</sub>)<sub>6</sub><sup>3+</sup> +M(e) + Ru(NH<sub>3</sub>)<sub>6</sub><sup>2+</sup> reaction for a variety of metal electrodes M.<sup>53</sup> The nonadiabatic expression for  $k_{el}^{ex}$  has a term proportional to the density of electronic states in the metal at the Fermi level, <sup>26,29</sup> and that density is, in turn, proportional to a coefficient  $\gamma$  in the temperature dependence of the electronic specific heat of the metal. If the ET reaction at M were adiabatic, however, the  $k_{el}^{ex}$  would be independent of the density of states and hence of  $\gamma$ . Experimentally,  $k_{el}^{ex}$  was found to be independent of  $\gamma$  when the latter was varied tenfold by varying the nature of the metal M, for the given redox system.<sup>53</sup>

Reactions which are required to occur over large distances, include those where the donor and acceptor in solution are separated by a long rigid saturated bridge  $^{54.57}$  or, are far apart in frozen media  $^{58}$ , or when they are far apart in proteins,  $^{59.62}$  or in an electrochemical system  $^{51}$  described below. All of these systems have a small matrix element  $H_{rp}$  and hence are clearly nonadiabatic. Nonadiabaticity is most clearly tested when, by varying the  $\Delta G^0$  in such systems, the value of the maximum rate can be measured (e.g., ref 93), namely at  $-\Delta G^0 \sim \lambda$ , and eq 13a then used to infer  $\kappa$ . An analogous example, but at an electrode interface M, occurred when the activation overpotential  $ne(E-E_0')$  was varied for a reaction where the redox agent was bound to a long chain molecule. The latter was part of an ordered monolayer of long chain molecules on the electrode surface. The maximum rate constant (an asymptote in a plot) showed that  $\kappa \nu$  was clearly much less than  $\nu$  and so the ET was clearly nonadiabatic in this case.

For reactions in solution when the reactants are moving freely rather than being held some fixed distance apart the problem of determining adiabaticity vs nonadiabaticity has been more difficult. For very fast reactions the high reaction rates which occur when  $-\Delta G^0 \sim \lambda$  tend to be masked by the slow and rate controlling diffusion of the reactants toward each other. For slower reactions the estimation of  $\kappa v$  from the pre-exponential factor of the bimolecular rate constant tends to be masked by other effects, such as the entropy associated with the work terms  $w_r$  and  $w_p$  (which were omitted for brevity in eq 13b) and any  $\Delta S^*$  associated with the reorganization in eq 48 given later. This  $\Delta S^*$  vanishes for isotopic exchange reactions, but the  $\Delta S$  associated with the w's remains. Some effort has been made to extract the  $\kappa v$  from such data, e.g., as in the MnO4 $^-$ -MnO4 $^-$ 

where  $\kappa$  appears to be about unity. A value of unity has been used for  $\kappa$  in the comparison noted in Section 3.1 of some absolute reaction rates with those calculated theoretically using eqs 13b and 23-27.4

### 3.8 ELECTRONIC MATRIX ELEMENTS

Recently many experiments have probed the dependence of the electronic matrix element  $H_{rp}$ , appearing in eq 40, on the distance and the nature of the medium separating the redox centers. A commonly employed technique has been to synthesize compounds with an electron donor D at one end, and an electron acceptor A at the other, with a covalently linked bridge B connecting the two: Here, intramolecular ÉT can take place from the donor to the acceptor. Usually a series of such compounds are synthesized where the donor and the acceptor groups are kept constant and the bridge length is systematically increased. The rate of ET is measured for the series. In order to infer values of relative electronic matrix elements from these values of rate constants, 1,63 one may proceed as follows:

It was seen in Section 1 that the rate constant  $k_r$  of a nonadiabatic ET

reaction (small  $H_{rp}$ ) is given by eq 41 as

$$k_r = \frac{2\pi}{\hbar} |H_{rp}|^2 \frac{1}{\left(4\pi\lambda k_B T\right)^{1/2}} \exp\left(-\Delta G^*/k_B T\right) \tag{45}$$

for an intramolecular process. Equation 45 can be written in the form

$$k_r = A \exp\left(-E_a/k_B T\right) \tag{46}$$

where  $E_a$  is the activation energy and A the pre-exponential factor. If the weak dependence of  $1/\sqrt{T}$  on T is neglected in eq 45, for purposes of the present lecture, we have

$$E_a \simeq \Delta H^{\bullet} \tag{47}$$

where  $\Delta H^*$  is the enthalpy term defined by the standard thermodynamic relation,  $\Delta H^* = \partial(\Delta G^*/T) / \partial(1/T)$ , since thermodynamic relations apply to these statistical mechanically defined kinetic quantities.

The pre-exponential factor A in eq 46 can then be written as

$$A \simeq \frac{2\pi}{\hbar} |H_{rp}|^2 \frac{\exp(\Delta S^*/k_B)}{\left(4\pi\lambda k_B T\right)^{1/2}}$$
 (48)

where  $\Delta S^*$  is equal to  $-\partial \Delta G^*/\partial T$ . Using eq 23 for  $\Delta G^*$ , we have

$$\Delta S^{\bullet} = \frac{1}{2} \left( 1 + \frac{\Delta G^{0}}{\lambda} \right) \Delta S^{0} \tag{49}$$

and

$$\Delta H^* = \frac{\lambda}{4} \left[ 1 - \left( \Delta G^0 / \lambda \right)^2 \right] + \frac{\Delta H^0}{2} \left[ 1 + \left( \Delta G^0 / \lambda \right) \right]$$
 (50)

assuming  $\lambda$  to be independent of temperature.

The  $\Delta S^0$  in eq 49 is zero for a self-exchange reaction. We also have  $\Delta S^0 = 0$  when the reactants in reaction 4 have charges on  $(Ox)_1$  and  $(Red)_2$  equal to those on  $(Ox)_2$  and  $(Red)_1$ , respectively, and when, in addition, the radii of the reactants 1 and 2 are about equal. When  $\Delta S^0$  is zero, it is seen from eq 49 that  $\Delta S^* = 0$ . It follows from eq 48 that A then provides a measure of  $|H_{rp}|^2$  for the series, there now being no  $\Delta S^*$  there. Again, if  $-\Delta G^0 \approx \lambda$ , it is seen from eqs 48 to 50 that  $\Delta S^* = 0$  and  $\Delta H^* = 0$ ,  $k_r = A$ , and that  $\Delta S^*$  is again absent from eq 48, permitting once more an estimate of  $|H_{rp}|^2$ .  $|H_{rp}|^2$  is also estimated more indirectly from  $E_a$  and A using eqs 47 to 50. One alternative route for determining the  $H_{rp}$ 's experimentally is to use charge-transfer (intervalence) spectra, upon introducing an approximation for the optical transition dipole matrix element. The latter is then proportional both to  $|H_{rp}|$  and to the separation distance between the donor and acceptor charges.

One procedure for calculating  $H_{rp}$  with theory is to seek the two lowest energy many-electron wavefunctions of the D-B-A system where the electronic charge is equally divided between D and A. Then the energy difference of these two delocalized many-electron states equals the  $2H_{rp}$  in Figure 3. This procedure can also be implemented more approximately using, instead, a one-electron description in which delocalized orbitals are formed from individual atomic orbitals localized on D and A. The energy difference between two delocalized orbitals equally distributed over D and A again gives  $H_{rp}$  but now

with the added one-electron approximation.

Alternatively, perturbation theory has been used to estimate  $H_{rp}$  by considering properties of the bridge and then treating the interaction of the donor and of the acceptor with the bridge using perturbation theory. In a simple case when the donor and the acceptor are each linked to one atomic orbital of the bridge,  $H_{rp}$  is given by  $^{68}$ 

$$H_{rp} = T_D T_A \sum_{\nu} \frac{C_{D\nu} C_{A\nu}}{b_{\nu} - a} \tag{51}$$

where  $T_D(T_A)$  are the matrix elements for interaction between D(A) and the adjacent atomic orbitals of the bridge,  $C_{i\nu}$  (i=D, A) is the coefficient of the bridge orbital  $\nu$  at the point of contact with i,  $b_{\nu}$  is the energy of the bridge orbital  $\nu$ , and a is the energy of the donor orbital. (The donor orbital and acceptor orbital have equal energies in the TS because of the influence of the environment, depicted in Figure 3.) Equation 51 may be extended to more general cases where D and A are both large groups with a number of orbitals connecting D(A) to B. Such a formalism in its one-electron or many-electron form has been termed "superexchange" in the literature, the electron making use of the orbitals of the bridge (both occupied and unoccupied) for electron transfer from D to A (or hole transfer from A to D).

For either of these calculational procedures, many-electron wavefunctions, all-electron SCF models, or semi-empirical methods may be

used to calculate the molecular orbitals and the energies required in the expression for  $H_{rp}$ . For large systems such as the biological systems to be discussed in the next section, at the present time, semi-empirical methods seem to offer the best alternative. Some examples of calculated values of  $H_{rp}$  (using the one-electron extended Hückel theory), along with experimentally determined values of  $H_{rp}$ , are given in Tables I-IV of ref 70. Encouraging agreement was found for the relative values of  $H_{rp}$  as a function of separation distance in each series.

### 3.9 EXTENSION TO BIOLOGICAL SYSTEMS

Metalloproteins have been extensively used to examine various aspects of ET reactions. 59-62 One important area of research has been to determine the electronic coupling provided by the protein medium. Both inter- and intramolecular protein electron transfer reactions have been investigated. As an example of the latter, a redox group such as [Ru(NH<sub>3</sub>)<sub>5</sub>]<sup>+3</sup> is covalently linked attached to a histidine (His) residue of a protein. Thus, Gray and coworkers have synthesized a series of ruthenium-modified proteins in which the donor and the acceptor are the same, but the ruthenium group is located in different residues of the protein, thus allowing distance and medium effects to be probed. In Figure 2 of ref 71, a myoglobin is illustrated in which there are four surface histidines, all of which can be singly ruthenated and the ET rate between the ruthenium-modified His and the metal porphyrin then measured. From the ratios of the square roots of these rates, ratios of the electronic matrix elements for the various derivatives can be obtained when any distance-dependent effect that may occur in FC, for example in the solvation effect on  $\Delta G^0$  and  $\lambda$ , is neglected. These values may be compared with ratios of the  $H_{rp}$  values calculated from a superexchange model (as in Table II of ref 72). The order of magnitude agreement between the relative calculated and experimental values is encouraging, and more detailed calculations including more amino acid residues of the proteins are in progress.

The photosynthetic charge transfer system is another area where there has been intense research in the last few years. The sequence of reactions is as follows: a) electronic excitation of the special bacteriochlorophyll pair, BChl2; b) transfer of electron from BChl2\* to a pheophytin, BPh, some 9-10 Å away in 2.8 picoseconds; c) transfer of electron from BPh- to a quinone QA in

the next 200 picoseconds.

The protein environment of BChl<sub>2</sub>, BChl and BPh is largely hydrophobic and therefore gives rise to a small  $\lambda_0$ . The vibrational  $\lambda_i$  is presumably also small since the bond lengths in the reactants (both in the large porphyrin rings of the chlorophyll molecules and the metal-ligand bond lengths) do not undergo much change in bond length upon electron gain or loss. Both aspects lead to an overall small reorganizational term,  $\lambda$ . The driving force of the formation of BPh- from BChl<sub>2</sub>\* also appears to be relatively small, around 0.2 eV, therefore allowing the forward reaction to proceed extremely rapidly, while minimizing loss of energy arising from the absorption of the sunlight. Further, the back ET from BPh- to form ground state BChl<sub>2</sub> appears to be extremely slow, perhaps due in part to an inverted effect, resulting in an efficient charge separation.

Another interesting question regarding these primary steps of photosynthesis that arises is the role of a nearby bacteriochlorophyll molecule

BChl in mediating the fast initial ET (e.g., refs 74-79). Direct ET from BChl<sub>2</sub>\* to BPh seems to be somewhat unlikely in view of the large separation between the two pigments. Other possibilities are a mechanism involving BChl<sup>-</sup> as an intermediate, or a superexchange mechanism where the BChl serves as a bridge. This topic is under active investigation and discussion.

### 4. Miscellaneous Questions

In these notes, we have attempted to include remarks on some of the questions raised in or out of class, such as how is the reaction coordinate of an electron transfer reaction is defined (refs 12 and 13), what, in detail, is the Landau-Zener theory for curve crossings (Appendix A), what justification is there for using the same "force constant" for the vibrations of the reactants as for the products (ref 20), how does one proceed from using potential energy surfaces to using free energy surfaces (Appendix A), why does  $\Delta G^0$  appear in the nonadiabatic rate expression when the initial Golden Rule formula on which it is based contains instead a  $\Delta E^0$  (ref 36), why is there no inverted effect in the electrochemical ET reactions at metal electrodes (Section 2.4), is there evidence for an exciplex formation, in the case of a fluorescence quenching ET reaction, which sometimes masks the inverted effect (ref 44), and what is the relation between long-range electron and triplet energy transfers (ref 94).

In this section, we address several additional questions which were

raised.

1. In the nonadiabatic equation for  $k_r$  is the  $(4\pi\lambda kT)^{1/2}$  factor part of an electronic factor or a nuclear factor?

The discussion of the Landau-Zener expression for "curve crossing" in Appendix A shows that this factor appears as a result of the  $\kappa(v)$  there, and so arises from the coupling of the electronic and nuclear motions. Thereby, it is to be assigned neither to the one nor to the other, but to both.

2. When  $\lambda \to 0$ , the nonadiabatic expression for  $k_r$  becomes infinite. Does this mean that  $k_r$  itself becomes infinite?

A value of  $k_r = \infty$  would be a physical impossibility. Rather, when the nonadiabatic ET expression, e.g., eq 41, becomes infinite when  $\lambda = 0$ , an assumption in which that equation is based has failed. In particular, the transition probability  $\kappa(v)$  in Appendix A is required to be small for the preexponential factor in eq 41 to be valid. In that Appendix  $\kappa(v)$  is shown there to be proportional to  $|H_{rp}|^2/\sqrt{\lambda}$ . However,  $\kappa(v)$  can no longer be small when  $\lambda$  approaches zero, and so a different formalism would be required.

3. What is the relation, if any, between electron tunneling and nuclear tunneling?

In Figures 3 and 9 potential energy curves are depicted for the nuclear motion and, as in Figure 9, can be used to describe nuclear tunneling. Not depicted in either of these plots is the many-dimensional surface  $V(\mathbf{r}_e)$  for the potential energy for the electrons as a function of the many electronic

coordinates re. The Schrödinger equation for the electronic wave function, holding the nuclei fixed at positions q (Born-Oppenheimer approximation), contains this  $V(\mathbf{r}_e)$ , and, when solved, provides an energy  $U(\mathbf{q})$ , which serves as the potential energy for the nuclear motion as a function of q in Figure 3. When the wave function is constrained to reside on the donor, this  $oldsymbol{U}$  becomes the surface  $U_r$ , and when it is constrained to reside instead on the acceptor, Ubecomes the  $U_p$  one. In the Schrödinger equation for the electrons, the region between the donor and the acceptor typically has a high potential energy  $V(r_e)$ for the electrons, so high that the electrons usually cannot penetrate that region classically. Nevertheless, ET does occur and, if one wishes to use the term, has occurred by electron tunneling from the donor to the acceptor.

Some measure of this electron "tunneling probability" during a typical period 1/v of nuclear motion (v being a typical frequency for that motion) can be obtained as follows: The frequency with which an electron would oscillate between two reactants whose nuclei were held fixed is shown below to be the Bohr frequency,  $2H_{rp}/h$ , where  $2H_{rp}$  is the splitting in Figure 3 due to the electronic interaction of the two reactants. The electron tunneling probability during the time  $1/\nu$  is then  $2H_{rp}/h\nu$ . For example, when  $H_{rp} \sim 100$  cm<sup>-1</sup> and  $\nu \sim 400$  cm<sup>-1</sup>, a typical metal-ligand frequency,  $2H_{rp}/h\nu \sim 1/2$ , and so the electron tunneling probability during a period  $1/\nu$  of the nuclear motion is  $\sim 1/2$  and the reaction is nearly "adiabatic." In some cases, however,  $H_{rp}$  is very small, the electron tunneling probability during the period 1/v is also therefore very

small, and the reaction is said to be "nonadiabatic.

In the case of a donor and acceptor separated by monomeric units in some bridge,  $H_{rp}$  decreases exponentially with an increase in the number N of monomeric units. Thereby, it decreases exponentially with increasing donoracceptor separation distance, when the chain of units is roughly linear. A semi-quantitative explanation is as follows: When there is one molecular orbital (empty in the case of electron transfer and occupied in the case of hole transfer) per unit, quantum mechanical perturbation theory shows that  $H_{rn}$ decreases by a factor  $V/\Delta E$  per unit, where V is the unit-to-unit electronic matrix element and  $\Delta E$  is the energy difference between the donor orbital and the unit's orbital. Thus, for N units,  $H_{rp}$  decreases by a factor  $(V/\Delta E)^N$ , i.e., by exp ( $-\beta R/2$ ), where R = Na, a being the length of a unit, and  $\beta = 2a^{-1} \ln (\Delta E/V)$ .

For an atom-atom matrix element of  $\sim 4$  to 5eV, a  $\Delta E$  of about the same value, and the product of the coefficients of the molecular orbitals on adjacent orbitals being about 1/20 when there are 20 relevant atoms per unit, the V is about (5/20) eV (cf. ref 95). When  $a \approx 5$  Å,  $\beta$  is then calculated to be about  $1.3\text{\AA}^{-1}$ , which is fairly close to a typical value<sup>70</sup> of  $\sim 0.7 \text{ Å}^{-1}$  to  $1 \text{ Å}^{-1}$ . (When there are 20 atoms contributing to a molecular orbital, each atomic coefficient is about  $1/\sqrt{20}$ .) The actual situation is more complicated in that a number of orbitals participate rather than merely one per unit, but the same exponential dependence on R prevails.

The connection between the above power rule,  $(V/\Delta E)^N$ , and eq 51 has been discussed by McConnell<sup>96</sup> for a particular case, in his treatment of triplet energy transfer in chain systems. A similar argument applies to electron

transfers.

## **4.** What is the relation between the splitting $2H_{rp}$ and the frequency of the electronic motion?

This relation can be seen as follows. Suppose that  $\psi_1$  denotes the electronic wave function when the electron is localized on the donor, and  $\psi_2$  when it is localized on the acceptor. The adiabatic wavefunctions, corresponding to the energies of the rounded-off curves at the intersection in Figure 3 would be  $(\psi_1 + \psi_2)/\sqrt{2}$  and  $(\psi_1 - \psi_2)/\sqrt{2}$ , with energies of  $U^* - H_{rp}$  and  $U^* + H_{rp}$ . Here  $U^*$  is the energy at the intersection  $U_r = U_p$ . If the electron is originally in the donor at time t=0, the electronic wavefunction  $\psi$  at any later time is

$$\psi = \frac{1}{2}(\psi_1 + \psi_2) \exp\left[-i(U^* - H_{rp})t/\hbar\right] + \frac{1}{2}(\psi_1 - \psi_2) \exp\left[-i(U^* + H_{rp})t/\hbar\right]$$
 (52)

 $\psi$  clearly equals  $\psi_1$  at t=0. At a time  $t=h/4H_{rp}$  it can be seen that  $\psi=\psi_2\exp i\theta$ , where  $\theta=-[(U^*/H_{rp})-1]\pi/2$ , i.e., that  $|\psi|^2=|\psi_2|^2$  and so the electron then resides on the acceptor. After a further time  $h/4H_{rp}$ ,  $|\psi|^2$  again equals  $|\psi_1|^2$ . Thereby, under conditions where the nuclei are fixed in position and the system is at the intersection of  $U_r$  and  $U_p$ , the electron would oscillate from donor to acceptor and back with a frequency of  $2H_{rp}/h$ . Since the nuclei move rather than stay fixed, an irreversibility actually occurs, described by the Landau-Zener expression in Appendix A or by more general treatments.

## 5. Are the potential energy surfaces parabolic for these and for other reactions?

We have noted that the PES for ET reactions are only parabolic (harmonic) along the vibrational coordinate axes. Along the solvational coordinates' axes they are highly anharmonic, with various local minima. The free energy plots, on the other hand, including both the solvational and vibrational contributions, are approximately harmonic functions of the reaction coordinate. Other transfer reactions are not represented well by parabolas for reactants and parabolas for products, even for the vibrational motion. In these reactions, a strong interaction of the reactants occurs, one bond is broken and another is formed, and so a quite different model should be used, one which takes account of these effects. One model which was developed leads to an energy barrier, which when phrased in potential energy terms, is given by 80

$$\Delta U^* = \frac{\lambda}{4} + \frac{\Delta U^0}{2} + \frac{\Delta U^0}{2\gamma} \ln \cosh \gamma \tag{53}$$

where  $y=(2\Delta U^0/\lambda) \ln 2$ ,  $\Delta U^0$  being the potential energy of reaction (difference of bond energies of reactants and products), and  $\lambda/4$  is the barrier at  $\Delta U^0=0$ . Further,  $\lambda_{12}=\frac{1}{2}(\lambda_{11}+\lambda_{22})$ , as in ET reactions. On In a region of  $|\Delta U^0/\lambda|$  of about 0 to 0.5, this equation is reasonably well approximated by the quadratic equation. However, in marked contrast to the latter, there is no inverted effect: in eq 53,  $\Delta U^*$  tends to zero monotonically when  $\Delta U^0/\lambda$  tends to minus infinity, as expected on physical grounds. It is the difficulty of intersection of

the two parabolas in Figure 8 at a conveniently small height which leads to the inverted effect.

### 6. Are proton transfers expected to display an inverted effect?

If the reactants were held so far apart that their interaction would be very weak, a parabolic picture for proton transfers would be adequate. Even in that case, however, the inverted effect would be difficult to observe: the proton levels are closely spaced ( $\sim$ 3,000 cm<sup>-1</sup> apart in OH or CH vibrations), in contrast with the usually wide spacing of electronic energy levels (typically ~30,000 cm-1). The possibility of forming electronically excited states of the reaction products, we have seen in Figure 8, opens new channels for reaction when the formation of the lower electronic state becomes inhibited because of the inverted effect. In the proton transfer case, the new channels would involve, instead, vibrationally excited states of the newly formed O-H, C-H, or N-H proton bond.

Typically, however, proton transfers are not expected to be represented well by the intersection of a pair of parabolas, and a strong interaction behavior, such as that depicted in the response to question 5, would be expected to lead to an equation similar to eq 53 rather than eq 11. On the other hand, in photoexcited proton transfer reactions in isolated systems at sufficiently low temperature (e.g., as in supersonic beams) a resonance might occur between the initial protonic energy level and the final one. Resonances provide the equivalent of a very narrow  $\ln k_r vs - \Delta G^0$  plot, with a sharp maximum. An equivalent behavior, but for an electronic transition, has been found in electric field controlled resonances in formaldehyde. 81 Perhaps under similar circumstances, an analogous effect can be made to occur for proton

transfers.

7. Is it meaningful to speak of the splitting of the free energy curves, as well as the PES?

The splitting  $2H_{rp}$  of the two PES depends mainly on the separation distance R and so, for a fixed R, is essentially constant along the intersection surface. Because of the relation between the free energy curves in Figure 4 and the PES in Figure 3, the splitting of the  $G_r(q)$  and  $G_p(q)$  curves is in that case essentially equal to  $2H_{rp}$  also. In other cases, if one wished to depict a splitting in Figure 4, that splitting would have to represent the value of  $H_{rp}$ , averaged over the intersection surface using a Boltzmann weighting factor.

### 8. Does recrossing of the intersection surface occur in the ET reaction?

Wigner has pointed out that if a "hypersurface" in phase space (i.e., a 2N-1 dimensional surface in a 2N-dimensional space which has N coordinates and N momenta as axes) could be found such that there were no recrossing of this hypersurface by classical trajectories of the system during the course of the reaction, classical mechanical transition state theory would be valid.82 The hypersurface is then the TS. The neglect of such recrossings in TS theory causes the TS calculated rate to be an upper bound to the actual reaction rate.

For an adiabatic reaction in solution, some recrossing probably occurs but typically relatively little, in the calculations of classical trajectories made thus far. The error in TS theory due to neglect of recrossings has been estimated by a large scale numerical calculation of classical trajectories of reactants in a particular  $S_N 2$  reaction<sup>83</sup> to be only a factor of about two. This error represents a relatively minor effect in reaction rate theories, which contain other approximations. One main task of such theories is to understand chemical effects which can sometimes vary by many orders of magnitude.

For nonadiabatic reactions, the smallness of  $\kappa(v)$  implies that most of the crossings of the  $U_r = U_p$  intersection surface will indeed not result in reaction, that is, in a transition from the  $U_r$  to the  $U_p$  surface. In such a case, after a crossing of the TS, the system will typically remain on the  $U_r$  surface, but will ultimately be reflected, and then recross the TS. However, such ineffectiveness to lead to a reaction is taken into account in the calculation of  $\kappa(v)$ , and no further correction of TS theory due to this source of recrossing is needed in this nonadiabatic case.

### 9. How does variational TS theory relate to the TS theory being used?

Following Wigner's ideas<sup>82</sup> on the implications of recrossings of the hypersurface, the most accurate choice of the hypersurface is the one for which there are the fewest recrossings. It can be shown that such a choice will be the one which gives the lowest calculated reaction rate, and thereby the rate closest to the actual rate. Selecting a TS, and varying it so as to obtain a minimum rate constant, is the essence of variational TS theory. In the case of ET reactions, use of the intersection surface for the TS is expected to provide the most straightforward choice for the TS.

### 5. Other Topics

There are many topics in the ET field which have been studied experimentally, and, in many cases, theoretically, including some of the topics listed in Figure 1 and not discussed here, such as solvent dynamics, with<sup>84</sup> and without<sup>85</sup> vibrational effects, electron transfer accompanied by rupture of a chemical bond,<sup>86</sup> electron transfer across the interface of two phases, either liquid-liquid,<sup>87</sup> liquid-polymer,<sup>88</sup> or polymer-polymer interfaces,<sup>89</sup> and many others. The field continues to expand in new directions and to offer a challenge to experimentalists and theoreticians alike.

### Acknowledgment

It is a pleasure to acknowledge the support of this work by the Office of Naval Research and by the National Science Foundation. A portion of these lectures was written while one of us (R.A.M.) was the Baker Lecturer at Cornell University. He is very pleased to acknowledge the hospitality and discussions of his colleagues there.

## Appendix A. Rate Expressions for Adiabatic and Nonadiabatic Reactions

The classical statistical mechanical expression for the rate constant can be written as

$$k_r = \int ... \int \dot{q}_1 \, \gamma \, \exp\left(-H(q_1^{\ddagger})/k_B T\right) dq_2...dq_N \, dp_1...dq_N / h^N Q$$
 (A1)

where  $q_1$  denotes the reaction coordinate (denoted by q in the text),  $H(q_1^{t})$  is the sum of the potential energy at the transition state (TS) plus the total kinetic energy (involving all N  $p_i$ 's), and  $\gamma$  is the probability of a successful electronic transition on reaching the TS (in our case going from the reactants to the products surface there, i.e., going from  $U_r$  to  $U_p$ ). The integral over  $p_1$  is from 0 to  $+\infty$  (rate in forward direction), the integrals over the remaining  $p_i$ 's are from  $-\infty$  to  $+\infty$ , and those over  $q_2...q_N$  are over the full range of these coordinates. Q is the partition function of the reactants

$$Q = \int ... \int \exp(-H/k_B T) dq_1...dq_N dp_1...dp_N/h^N$$
 (A2)

H being the sum of the kinetic and potential energy of the reactants and solvent molecules.

Equation A1 was obtained by using an expression for the probability density of finding the system at  $q_1^{\dagger}$  (per unit length along  $q_1$ ), multiplying by the velocity  $\dot{q}_1$  along the reaction coordinate to obtain the probability flux, then multiplying by  $\gamma$  to obtain the reaction probability flux, and integrating over the coordinates at fixed  $q_1(=q_1^{\dagger})$  and over the momenta as indicated.

When  $\gamma$  is unity in the range of coordinates and momenta of interest, use of a classical mechanical equation  $\dot{q}_i = \partial H/\partial p_i$ , and integration over  $p_1$  and over the remaining variables in eq A1 yields the standard TS theory expression for  $k_r$  for an adiabatic reaction ( $\gamma = 1$ ), treated classically:

$$k_r = \frac{k_B T}{h} \frac{Q^{\ddagger}}{Q} \exp\left(-\Delta U^{\ddagger} / k_B T\right) \tag{A3}$$

where  $\Delta U^{\dagger}$  denotes the lowest potential energy of  $U_r$  in the TS minus that of  $U_r$  anywhere, and where  $Q^{\dagger}$  is the partition function for the transition state:

$$Q^{\ddagger} = \left[ \dots \right] \exp \left[ -H(q_1 = q_1^{\ddagger}, p_1 = 0)/k_B T \right] dq_2 \dots dq_N dp_2 \dots dp_N/h^{N-1}$$
 (A4)

The H in eq A4 is now the sum of the potential energy of the TS, measured relative to the lowest value on the TS, plus the kinetic energy of the TS.

Q is seen from eqs A2 and A4 to contain one coordinate and one momentum,  $q_1$  and  $p_1$ , more than  $Q^{\ddagger}$ . Upon integration in eq A2 over all  $q_i$  and  $p_i$  but  $q_1$  and  $p_1$ , one obtains for Q for a unimolecular reaction a factor given later by eq B2 and denoted by  $\exp{[-G_r(q_1)/k_BT]}$ ,  $G_r(q_1)$  being the "reorganizational" free energy as a function of  $q_1$ . It is approximately a

quadratic function of  $q_1$ , as discussed earlier in the text (linear response approximation). When the integral of this factor over  $q_1$  is combined with the integral over  $p_1$ , one obtains a factor which is approximately equal to a classical vibrational partition function,  $k_BT/h_V$ , where v is a typical frequency associated with this motion along the reaction coordinate  $q_i$ . If Q' denotes the remaining factor in Q,  $Q/(k_BT/h_V)$ , we then have

$$k_r = \nu \frac{Q^{\dagger}}{Q'} \exp\left(-\Delta U^{\dagger} / k_B T\right) \tag{A5}$$

The term  $(Q^{\dagger}/Q')$  exp  $(-\Delta U^{\dagger}/k_BT)$  in eq A5 can be written as the exp  $(-\Delta G_r^{\bullet}/k_BT)$  in the text and is associated, at the separation distance R, with the solvational and vibrational reorganization needed to reach the TS. From eq A5 we then obtain eq 13a of the text for a unimolecular reaction, with  $\kappa=1$ .

For bimolecular reactions, three of the coordinates in eq A1 can be chosen to be the center of mass of the two reactants. The contribution of these coordinates and their momenta to the integral in eq A1 just cancels their contribution in eq A2. Three of the remaining coordinates can be chosen to be the relative coordinates of the two reactants. To conform to the definition of a bimolecular reaction rate constant, the integration over these relative coordinates in Q in eq A2 is over a unit volume. If in eq A1 the electron transfer rate has a  $\gamma$  which decreases with separation distance R as exp  $[-\beta(R-R_0)]$  and which equals approximately unity at contact  $(R=R_0)$ , integration over the three coordinates in the integral in eq A1 yields a factor  $\int 4\pi \tilde{R}^2 \exp\left[-\beta(R-R_0)\right] dR$ , which is well approximated by  $4\pi \tilde{R}_0^2/\beta$ , since  $\beta^{-1} < < R$ . This term is the  $v_s$  in eq 13b in the text. The momentum contribution to Q' and to  $Q^{\dagger}$  in eq A5 for these translational coordinates cancels. The remaining contributions to  $Q^{t}$  and Q are the same as those for unimolecular reactions, and yield, as in the unimolecular case, the reorganizational factor exp  $(-\Delta G_r^*/k_BT)$ . Thereby, one obtains eq 13b of the text with  $\kappa=1$ . Under some conditions the R in the TS may not equal the separation distance  $R_0$  at point of contact  $R_0$ , and  $\Delta G_r^*$  and  $\kappa$  are then computed at the R for the TS. (The rate depends on R through  $\kappa$  and through  $\Delta G_r$ , and its maximum could occur at an R somewhat greater than  $R_0$ .)

For reactions at an electrode related considerations apply. Now, three of

For reactions at an electrode related considerations apply. Now, three of the coordinates in Q and in  $Q^{\ddagger}$  in eq A3 are the translational coordinates of the reactant. In conformity with the definition of  $k_r$  for such a reaction, the three coordinates in Q are integrated over a unit volume. Two of them in  $Q^{\ddagger}$  are integrated over a unit area of the electrode, while the third coordinate, the coordinate z, which is perpendicular to the electrode surface, contributes a factor to  $Q^{\ddagger}$  of  $\int \exp(-\beta z)dz$ , the integral being from z=0, the point of contact with the electrode, to  $z=\infty$ . Thereby one obtains  $\beta^{-1}$ , which is the  $v_e$  in eq 33a in the text. The remaining contributions to eq A3 are the same as above, and so

one obtains eq 33a of the text, with  $\kappa = 1$ .

We turn next to highly nonadiabatic reactions, i.e., when  $\gamma < 1$  in eq A1 in the coordinate and momentum region of interest. A one-dimensional approximation to  $\gamma$  is given by the Landau-Zener expression:<sup>17</sup>

$$\gamma = 1 - e^{-\kappa(v)} \tag{A6}$$

where

$$\kappa(v) = \frac{2\pi}{\hbar} \frac{|H_{rp}|^2}{v|s_r - s_p|} \tag{A7}$$

Here, v is the velocity  $\dot{q}_1$  along the reaction coordinate at the intersection of the two potential energy curves (at  $q_1=q_1^{\dagger}$  in our case), and  $s_r$  and  $s_p$  are the slopes of the potential energy curves at the intersection,  $\partial U_r/\partial q_1$  and  $\partial U_p/\partial q_1$  in the present case. Strictly speaking, eqs A6 and A7 were derived for a one-coordinate system. If applied, nevertheless, to the present many-coordinate case, these slopes depend on the point  $(q_2,...q_N)$  being crossed at  $q_1=q_1^{\dagger}$ . If some mean value for the slopes is used (since there is an integration in eq A1 over  $q_2...q_N$ ), e.g., if we assume  $U_r$  to be approximately  $\frac{1}{2}k$   $(q_1-q_1^{r})^2$  plus terms independent of  $q_1$ , and  $U_p$  to be  $\frac{1}{2}k$   $(q_1-q_1^{p})^2$  plus terms independent of  $q_1$ , then  $|s_r-s_p|$  equals  $|k(q_1^{r}-q_1^{p})|$ . If we regard  $\lambda$  as being approximately  $\frac{1}{2}k(q_1^{r}-q_1^{p})^2$ , as in the text, then  $|s_r-s_p| = \sqrt{(2k\lambda)}$ . If we consider the case that  $\kappa(v) < 1$  in the region of interest, then in eq A6  $\gamma = \kappa(v)$ . The velocity v in the denominator of eq A7 then cancels the  $\dot{q}_1$  in eq A1. If the kinetic energy in H in A1 is regarded as being  $\frac{1}{2}p_1^{2}/\mu_1$  plus terms independent of  $p_1$ , integration of eq A1 then yields

$$k_r = \frac{2\pi}{\hbar} \frac{|H_{rp}|^2}{(4\pi\lambda k_B T)^{1/2}} \frac{Q^{\dagger}}{Q'} \exp(-\Delta U^{\dagger}/k_B T)$$
 (A8)

upon once again extracting the factor  $k_BT/h\nu$  from Q and also using the

relation  $\sqrt{(k/\mu)} = 2\pi\nu$ . Two v's then cancel.

The term  $(Q^{\dagger}/Q')$  exp  $(-\Delta U^{\dagger}/k_BT)$  in eq A8 equals exp  $(-\Delta G_r^{*}/k_BT)$  for unimolecular reactions as before, while for bimolecular reactions and electrode reactions in which the reactant is not bound to the electrode, it equals  $v_s$  exp  $(-\Delta G_r^{*}/k_BT)$  and  $v_e$  exp $(-\Delta G_r^{*}/k_BT)$ , respectively, where  $v_s$  and  $v_e$  were defined above. The  $|H_{rp}|$  in eq A8 now denotes the matrix element when the two reactants (or the reactant and the electrode) are in contact.

In this way, in the case of very small  $\gamma$ , eqs 13 and 33 of the text are obtained, but with  $\kappa\nu$  being given in each case by eq 14b in the text. For intermediate values of  $\gamma$ , one could either integrate eq A1 using eq A6, or simply interpolate approximately by using eq 14b when the right-hand side of

eq 14b is less than v and then using eq 14a otherwise.

Physical insight into eq A7 in terms of the "frequency" of the electronic motion in the TS, obtained as  $2H_{rp}/h$  in Section 4, namely the separation of the adiabatic energy levels in the TS in Figure 3 divided by h, and of an effective frequency for the nuclear motion in the vicinity of the "crossing point" is given in ref 90.

### Appendix B. The Reorganizational Free Energy G(q)

The expression for G(q), the free energy of reorganization as a function of q, is considered next. (q is the reaction coordinate denoted by  $q_1$  in Appendix A.) We consider unimolecular reactions first. Using classical statistical mechanics, we have

$$\exp[-G(q)/k_BT] = \int ... \int \exp[-H(q_1 = q, p_1 = 0)/k_BT] dq_2...dq_N dp_2...dp_N/h^{N-1}$$
(B1)

The kinetic energy term in H in eq B1 is of the form  $\frac{1}{2}\sum_{i,j}g^{ij}p_ip_j$ . With this quadratic form, a standard expression on the used to evaluate the integral in eq B1 over  $p_2$  to  $p_N$ . If the determinant of the  $g^{ij}$ 's, for i and j not equal to 1, is denoted by 1/g', then we have upon integration of the  $p_i$ 's

$$\exp[-G(q)/k_BT] = \frac{\left(2\pi k_B T\right)^{(N-1)/2}}{h^{(N-1)}} \int \exp[-U(q_1=q)/k_B T] dS$$
 (B2)

where dS denotes the N-1-dimensional volume element  $\sqrt{g'dq_2...dq_N}$ . Apart from a prefactor, eq B2 is the same as eq 5 in the text, upon introducing r

subscripts.

Where the reaction being considered is bimolecular or when it involves an ET between an ion in solution and an electrode, there are also translational coordinates to be considered, as noted in Appendix A. The G(q) given by eq B1 or B2 is then intended to be the value when the reactants are held fixed at some separation distance R, and is a function of that R. In this case, some of the N-1 coordinates would be the translational coordinates of the reactants and the G(q) would be defined with eq B1, but using a number of coordinates less than the N-1 there, less by the number of translational coordinates of the reactants, six in the bimolecular case, and three in the case of the electrode reaction.

# Appendix C. Comparison of Quantum Expressions and Remarks on $\ln k_r$ vs $-\Delta G^0$ Asymmetry

It is instructive to examine the limiting situation for eqs 42 and 43 when  $\lambda_0 \rightarrow 0$  and when both  $T \rightarrow 0$  and  $\lambda_0 \rightarrow 0$ , and to see how the two expressions become identical there. At sufficiently low temperatures, reaction occurs only from the lowest vibrational energy level (no other level is populated), a situation which is obtained in eq 42 by letting  $T \rightarrow 0$ . Equation 42 then becomes

$$k_r = \frac{2\pi}{\hbar} |H_{rp}|^2 e^{-S} S^m / \Gamma(m+1) hv$$
 (T=0) (C1)

where  $\Gamma(m+1)$  is the Gamma function (= m! when m is an integer) and m=

 $-\Delta G^0/h\nu$ , defined here for  $m \ge 0$ .

Equation 43a can be expected to approach eq C1, and eq 43b to approach eq 42, only when the  $\lambda_o$  in eqs 43a and 43b is made to approach zero, since eqs C1 and 42 contain no  $\lambda_o$  contribution. When  $\lambda_o$  approaches zero, the function  $(4\pi\lambda_o k_B T)^{-1/2} \exp\left[-(\lambda_o + \Delta G^0 + mh\nu)^2/4\lambda_o k_B T\right]$  becomes extremely small, when regarded as a function of  $\Delta G^0 + mh\nu$ , except at  $\Delta G^0 + mh\nu = 0$ . (The effect of the  $\lambda_o$  in the denominator of the exponent dominates that in the preexponential factor.) Indeed, in the limit of  $\lambda_o \to 0$ , this function becomes a Dirac

delta function  $\delta(\Delta G^0 + mh\nu)$ . Thereby, eq 43a in this limit becomes

$$k_r = \frac{2\pi}{\hbar} |H_{rp}|^2 \sum_{m=0}^{\infty} \delta(\Delta G^0 + mhv) e^{-S} S^m / \Gamma(m+1)$$
 (C2)

where the m! in eq 43a has been written as  $\Gamma(m+1)$ . The derivation of the nonadiabatic expressions, eqs 42 and 43a, is based on the use of Fermi's Golden Rule, which in turn considers transitions from the initial state to a continuum of final states which are quasi-degenerate with the initial state and so preserve conservation of energy in the reaction step. In eq C2, this degeneracy can only occur if hv were regarded as small enough that the sum over m becomes a sum over a continuum, i.e., becomes an integral over dm. If we then use the wellknown relation that  $\delta(\Delta G^0 + mh\nu)$  equals  $(1/h\nu)\delta([\Delta G^0/h\nu] + m)$ , and the integral over m is evaluated, it follows that eq C2 reduces to eq C1. Thus, at low temperatures and at  $\lambda_0 = 0$ , eqs 42 and 43a become the same expression, as expected. A similar argument shows that, at any temperature, when  $\lambda_0$  tends to zero, eq 43b reduces to eq 42.

In concluding this Appendix, we comment briefly on the dependence of expressions such as eq C1 on the temperature in the inverted region. Introducing Stirling's formula for  $\Gamma(m+1)$ ,  $(m/e)^m \sqrt{(2\pi m)}$ , it is seen that  $\ln k_r$ varies with m as m In  $(Se/m) - \ln \sqrt{(2\pi m)}$ . Since a logarithmic dependence on m is a rather weak one, the principal dependence of  $\ln k_r$  on m, and hence on  $-\Delta G^0$ , is seen to be a linear one, with a slope  $\gamma = \ln (\lambda e/|\Delta G^0|)$ . Thus, the dependence of  $\ln k_r$  on  $-\Delta G^0$  in this quantum treatment is essentially linear

rather than quadratic.

### References

1. Marcus, R. A. and Sutin, N. (1985) Biochim. Biophys. Acta., 811, 265.

2. J. R. Bolton, N. Mataga and G. McLendon (eds.)(1991) Adv. Chem. Ser., 228, assorted articles.

3. Newton, M. D. and Sutin, N. (1984) Ann. Rev. Phys. Chem., 35, 437.

4. Sutin, N. (1983) Prog. Inorg. Chem., 30, 441.

5. Newton, M. D. (1991) Chem. Rev., 91, 767.

6. Cannon, R. D. (1980) Electron Transfer Reactions, Butterworths, London.

7. Eberson, L. (1987) Electron Transfer Reactions in Organic Chemistry, Springer, New York.

8. Fox, M. A. and Chanon, M. (eds.) (1988) Photoinduced Electron

Transfer, Elsevier, New York. 4 vols.

9. Twigg, M. V. (ed.) (1991) Mechanisms of Inorganic and Organometallic Reactions, vol. 7, Chaps. 1 and 2, and earlier

10. Brunschwig, B. S., Logan, J., Newton, M. D. and Sutin, N. (1980) J. Am. Chem. Soc., 102, 5798.

11. Sutin, N. (1988) Pure & Appl. Chem., 60, 1817.

12. King, G. and Warshel, A. (1990) J. Chem. Phys., 93, 8682.

13. Marcus, R. A. (1960) Disc. Faraday Soc., 29, 21. 14. Marcus, R. A. (1956) J. Chem. Phys., 24, 966.

15. Marcus, R. A. (1965) J. Chem. Phys., 43, 679.

16. Kuharski, R. A., Bader, J. S., Chandler, D., Sprik, M., Klein, M. S. and Impey, R. W. (1988) J. Chem. Phys., 89, 3248; Hwang, J.-K. and Warshel, A. (1987) J. Am. Chem. Soc., 109, 715.

17. Landau, L. (1932) Phys. Z. Sowjetunion, 1, 88; 2, 46; Zener, C. (1932)

Proc. Roy. Soc., 137A, 696; 140A, 660. See also ref 90 below.

18. Marcus, R. A. (1964) Ann. Rev. Phys. Chem., 16, 155. 19. Marcus, R. A. (1981) Int. J. Chem. Kinetics, 13, 865.

20. Since the value of k<sub>i</sub> will differ before and after the ET, it is often approximated as a particular average of the value for the reactants' ith mode, k<sub>i</sub><sup>r</sup> and the value for the products' ith mode, k<sub>i</sub><sup>p</sup>: k<sub>i</sub> = 2k<sub>i</sub><sup>r</sup> k<sub>i</sub><sup>p</sup> /(k<sub>i</sub><sup>r</sup> + k<sub>i</sub><sup>p</sup>). This step has been called "symmetrizing" the PES. Calculations have been made showing that this approximation. (Marcus, R. A. (1987) in A. E. Hansen, J. Avery and J. P. Dahl (eds), Understanding Molecular Properties, Reidel, Boston, p. 229.)

21. Marcus, R. A. (1965) J. Chem. Phys., 43, 58.

22. Marcus, R. A. (1965) J. Chem. Phys., 43, 3477, Appendix I.

23. Marcus, R. A. (1965) J. Chem. Phys., 43, 1261.

24. Cannon, R. D. (1977) Chem. Phys. Lett., 49, 299.

- 25. Brunschwig, B. S., Ehrenson, S. and Sutin, N. (1986) J. Phys. Chem., 90, 3657.
- 26. Dogonadze, R. R. (1971) in Hush, N. S. (ed), Reactions of Molecules at Electrodes, Wiley, New York, Chap. 3, Eq. 201.

27. Sumi, H. (1980) J. Phys. Soc. Jpn., 49, 1701; Sumi, H. and Marcus, R. A. (1986) J. Chem. Phys., 84, 4894.

28. Marcus, R. A. (1977) in P. Å. Rock (ed.), Special Topics in Electrochemistry, Elsevier, New York, p. 161; Marcus, R. A. (1959) Can. J. Chem. 37, 155.

29. Levich, V. G. and Dogonadze, R. R. (1959) Dokl. Acad. Nauk SSSR, 124, 123; Dogonadze, R. R., Kuznetsov, A. M. and Vorotyntsev, M. A. (1972) Phys. Stat. Sol. B, 54, 125, 425; Levich, V. G. (1970) in Eyring, H. (ed.), Physical Chemistry, An Advanced Treatise, Academic, New York, Vol. 9, Chap. 12.

30. Marcus, R. A. (1963) J. Phys. Chem., 67, 853, 2889.

31. Marcus, R. A. (1965) J. Chem. Phys., 43, 2654; (1970) 52, 2803.

32. Wallace, W. L. and Bard, A. J. (1979) J. Phys. Chem., 83, 1350.

33. Kestner, N. R., Logan, J. and Jortner, J. (1974) J. Phys. Chem., 78, 2148; Ulstrup, J. and Jortner, J. (1975) J. Phys. Chem., 63, 4358; Efrima, S. and Bixon, M. (1976) Chem. Phys., 13, 447; Siders, P. and Marcus, R. A. (1981) J. Am. Chem. Soc. 103, 741, 748.

34. Marcus, R. A. and Siders, P. (1982) J. Phys. Chem., 86, 622.

35. Warshel, A. (1982) J. Phys. Chem., 86, 2218.

36. Marcus, R. A. (1984) J. Chem. Phys., 81, 4494.

37. Kober, E. M., Casper, J. V., Lumpkin, R. S. and Meyer, T. J. (1986) J. Phys. Chem. 90, 3722; Chen, P., Duesing, R., Graff, D. K. and Meyer, T. J. (1991) ibid. 95, 5850.

38. Engleman, R. and Jortner, J. (1970) Mol. Phys. 18, 145.

39. Liang, N., Miller, J. R. and Closs, G. L. (1990) J. Am. Chem. Soc. 112, 5353.

40. E.g., Landau, L. D. and Lifshitz (1958) Quantum Mechanics,
Pergamon Press, New York, eq 51.6, and analogous arguments for
the case where the slopes are of opposite sign in the tunneling
region; Child, M. S. (1991) Semiclassical Mechanics With Molecular
Application, Clarendon Press, New York, eq (5.120) with α=0 there.

41. Li, T. T.-T. and Brubaker Jr., C. H. (1981) J. Organomet. Chem., 216,

223.

42. Powers, J. M. and Meyer, T. J. (1980) J. Am. Chem. Soc., 102, 1289; Callahan, R. W. and Meyer, T. J. (1976) Chem. Phys. Lett., 39, 82.

43. Rehm, D. and Weller, A. (1970) Isr. J. Chem., 8, 259; Nagle, J. K., Dresick, W. J. and Meyer, T. J. (1975) J. Am. Chem. Soc., 97, 2909; Scandola, F. and Balzani, V. (1979) J. Am. Chem. Soc., 101, 6140.

44. Kikuchi, K., Takahashi, Y., Katagiri, T., Niwa, T. and Hoshi, M. (1991) Chem. Phys. Lett., 180, 403; Kikuchi, K., Takahashi, Y., Hoshi, M., Niwa, T., Katagiri, T. and Miyashi, T. (1991) J. Phys. Chem. 95, 2378.

45. Miller, J. R., Closs, G. L. and Calcaterra, L. T. (1984), J. Am. Chem.

Soc., 106, 3047.

46. Gould, I. R., Mueller, L. J. and Farid, S. (1991) Z. Phys. Chem., 170, 143; Gould, I. R., Ege, D., Moser, J. E. and Farid, S. (1990) J. Am. Chem. Soc., 112, 4290, and references cited therein.

47. Asahi, T., Mataga, N., Takahashi, Y., Miyashi, T. (1990) Chem. Phys.

Lett., 171, 309, and references cited therein.

48. Gaines, G. L., O'Neil, N. P., Svec, W. A., Niemczyk, M. P. and Wasielewski, M. R. (1990) J. Am. Chem. Soc., 13, 719, and references cited therein.

49. Fox, L. S., Kozik, M., Winkler, J. R. and Gray, H. B. (1990) Science

**247**, 1069.

50. Penner, R. M., Heben, M. J., Longin, T. L. and Lewis, N. (1990) Science, 250, 1118; private communication.

51. Chidsey, G. E. (1991) Science, 251, 919.

52. Savéant, J. M. and Tessier, D. (1982) Faraday Disc. Chem. Soc., 74, 57; Weaver, M. J. and Hupp, J. T. (1982) Am. Chem. Soc. Symp. Series, 198, 181.

53. Iwasita, T., Schmickler, W., and Schultze, J. W. (1985) Ber.

Bunsenges. Phys. Chem., 89, 138.

54. Isied, S. S., Vassilian, A., Magnuson, R. H. and Schwarz, H. A. (1985) J. Am. Chem. Soc., 107, 7432; Vassilian, A., Wishart, J. F., van Hemelyrck, B, Schwarz, H. and Isied, S. S. (1990) J. Am. Chem. Soc., 112, 7278.

55. Closs, G. L., Calcaterra, L. T., Green, N. J., Penfield, K. W. and Miller, J. R. (1986) J. Phys. Chem., 90, 3673.

- 56. Penfield, K. W., Miller, J. R., Paddon-Row, M. N., Cotsaris, E., Oliver, A. M. and Hush, N. S. (1987) J. Am. Chem. Soc., 109, 5061.
- 57. Wasielewski, M. R., Niemczyk, M. P., Johnson, D. G., Svec, W. A. and Minsek, D. W. (1989) Tetrahedron, 45, 4785.

58. Beitz, J. V. and Miller, J. R. (1979) J. Chem. Phys., 71, 4579.

59. Isied, S. S. (1984) Prog. Inorg. Chem., 32, 443.

60. Bowler, B. E., Raphael A. L. and Gray, H. B. (1990) Prog. Inorg. Chem., 38, 259.

61. Sykes, A. G. (1991) Adv. Inorg. Chem., 36, 377.

- 62. Hoffmann, B. M., Natan, M. J., Nocek, J. M. and Wallin, S. A. (1991) Struct. Bond., 75, 85.
- 63. Isied, S. S., Vassilian, A., Wishart, J. F., Creutz, C., Schwarz, H. A. and Sutin, N. (1988) J. Am. Chem. Soc., 110, 635.
- 64. Hush, N. S. (1967) Prog. Inorg. Chem., 8, 391.
- 65. Hopfield, J. J. (1977) Biophys. J., 18, 311.
- 66. Creutz, C. (1983) Prog. Inorg. Chem., 30, 1.
- 67. Stein, C. A., Lewis, N. A. and Seitz, G. J. (1982) J. Am. Chem. Soc., 104, 2596.
- 68. McConnell, H. M. (1961) J. Chem. Phys., 35, 508.
- 69. Larsson, S. (1981) J. Am. Chem. Soc., 103, 4034.
- 70. Siddarth, P. and Marcus, R. A. (1990) J. Phys. Chem., 94, 2985.
- 71. Axup, A. W., Albin, M., Mayo, S. L., Crutchley, R. J. and Gray, H. B. (1988) J. Am. Chem. Soc., 110, 435.
- 72. Siddarth, P. and Marcus, R. A. (1990) J. Phys. Chem., 94, 8430.
- 73. For a recent review, see Kartha, S. Das, R. and Norris, J. R. (1991), in H. Sigel (ed.), Metal Ions in Biological Systems, 27, 323.
- 74. Breton, J. and Vermeglio, A. (eds.) (1988) The Photosynthetic Bacterial Reaction Center--Structure and Dynamics, NATO ASI Series A: Life Sciences 149, Plenum, New York.
- 75. Michel-Beyerle, M. E. (ed.) (1985) Antennas and Rection Centers of Photosynthetic Bacteria, Springer, Berlin
- 76. Holzapfel, W., Finkele, U., Kaiser, W., Oesterhelt, D., Scheer, H., Stilz, H. U. and Zinth, W. (1990) Proc. Natl. Acad. Sci. U.S.A., 87, 5168.
- 77. Kirmaier, C. and Holten, D. (1990) Proc. Natl. Acad. Sci. U.S.A., 87, 3552.
- 78. Plato, M., Mobius, K., Michel-Beyerle, M. E., Bixon, M. and Jortner, J. (1988) J. Am. Chem. Soc., 110, 7279.
- 79. Marcus, R. A. (1988) Isr. J. Chem. 28, 205.
- 80. Marcus, R. A. (1968) J. Phys. Chem. 72, 891.
- 81. Polik, W. F., Guyer, D. R. and Moore, C. B. (1990) J. Chem. Phys. 92, 3453.
- 82. Wigner, E. (1938) Trans. Faraday Soc. 34, 29.
- 83. Bergsma, J. P., Gertner, B. J., Wilson, K. R. and Hynes, J. T. (1987) J. Chem. Phys. 86, 1356.
- 84. Sumi, H. and Marcus, R. A. (1986) J. Chem. Phys. 84, 4894; Nadler, W. and Marcus, R. A. (1987) *ibid.* 86, 3906.
- 85. Susman, L. D. (1980) Chem. Phys. 49, 295; Helman, A. B. (1982) *ibid*. 65, 271; Calef, D. F. and Wolynes, P. G. (1983) J. Phys. Chem. 87, 3387; van der Zwan, G. and Hynes, J. J. (1985) *ibid*. 89, 4181.
- 86. Savéant, J.-M. (1987) J. Am. Chem. Soc. 109, 6788.
- 87. Marcus, R. A. (1990) J. Phys. Chem. 94, 4152, 7742; Marcus, R. A. (1991) J. Phys. Chem. 95, 2010; Geblewicz, G. and Schiffrin, D. J. (1988) J. Electroanal. Chem. 244, 27.
- 88. Leidner, C. R. and Murray, R. W. (1984) J. Am. Chem. Soc. 103 1606.
- 89. Leidner, C. R. and Murray, R. W. (1985) J. Am. Chem. Soc. 107, 551; Jernigan, J. C. and Murray, R. W. (1990) *ibid.*, 112, 1034.
- 90. Kauzmann, W. (1957) Quantum Chemistry, Academic Press, New York, p. 539.

91. Bellman, R. (1960) Introduction to Matrix Analysis, McGraw Hill, New York, p. 96.

92. Marcus, R. A. (1989) J. Phys. Chem. 93, 3078.

93. Moser, C. C., Keske, J. M., Warncke, K., Farid, R. S. and Dutton, P. L. (1992) Nature 355, 796.

94. Johnson, M. D., Miller, J. R., Green, N. S. and Closs, G. L. (1989) J. Am. Chem. Soc. 111, 3751.

95. Siddarth, P. and Marcus, R. A. (1992) J. Phys. Chem. 96, 000.

96. McConnell, H. M. (1960) J. Chem. Phys. 33, 115.

97. An alternative discussion of the solvent reorganization in terms of charges and potentials instead of in terms of electric fields and polarization vectors is given in the first citation of ref. 28.